Table of contents

Riassunto *3*

Abstract *6*

Introduction *9*

Toxins and lipids 9
The neuromuscular junction as a target for many toxins 10
Lipids role on synaptic vesicle fusion 12
Toxins acting on lipids: the snake PLA2 family 16
Classification and structural organisation 16
SPANs neurotoxicity and enzymatic activity 18
Features of paralysis induced by SPANs in NMJ models 22
Equivalent effect of toxins and their lipidic products 25
Mouse neuromuscular junction 26
Neuronal cell models 28
Other inverted-cone shaped lipids 31

Materials and methods *33*

Materials 33
Lipids preparation 33
Mouse phrenic nerve-hemidiaphragm preparation 34
Cell cultures 34
Calcium imaging 35
Viability assay 36
Fly stocks 36
Electrophysiology 36
Immunohistochemistry 37
Toxin Labelling and Assay 38
Assessment of Permeability Transition in Isolated Mitochondria 38

Results and discussion *40*

Effects of different lysophospholipids on the neuromuscular junction 40
Reversibility of lysoPLs induced paralysis of the neuromuscular junction 44
Comparison of SPANs and their lipid products at the Drosophila melanogaster larval neuromuscular junction 46

Role of salivary lipids and PLA2 activity in insect..... 49
Intracellular calcium increase induced by SPANs and lipid mixtures 51
Involvement of mitochondria in the mechanism of SPANs action 55
Paralysis of the neuromuscular junction induced by miltefosine, perifosine and lysoPAF..... 57
Morphological alteration produced on cellular models by inverted-cone shaped lipids..... 59
Effect of miltefosine, perifosine and lysoPAF on intracellular calcium levels and cellular vitality 62

Conclusions..... 66

References..... 68

Riassunto

Il veleno di molti serpenti contiene neurotossine ad azione presinaptica (**SPAN**, snake presynaptic PLA2 neurotoxin) che sono in grado di provocare blocco della neurotrasmissione e paralisi muscolare. I motivi strutturali sono molto conservati, ma la struttura quaternaria è molto variabile; si sono perciò prese in considerazione quattro tossine di diversa complessità strutturale: notexin (monomero), β-bungarotoxin (eterodimero), taipoxin (trimero) e textilotoxin (pentamero).

Queste tossine sono dotate di attività enzimatica di tipo PLA2, cioè idrolizzano il legame estereo in posizione 2 dei glicerofosfolipidi, producendo lisofosfolipidi e acidi grassi.

Utilizzando miscele equimolari di questi lipidi su giunzione neuromuscolare isolata e su neuroni in coltura si è dimostrato che essi sono in grado di riprodurre gli effetti delle tossine: blocco della neurotrasmissione con alterazione della morfologia dei terminali (deplezione delle vescicole sinaptiche, rigonfiamento, alterazione dei mitocondri) e formazione di rigonfiamenti ("bulges") sui neuriti, caratterizzati da accumulo di proteine specifiche delle vescicole sinaptiche. Questi dati hanno portato a interpretare il meccanismo d'azione delle tossine come uno sbilanciamento tra eso ed endocitosi, dovuto alle caratteristiche strutturali dei lipidi che vengono prodotti: la lisofosfatidilcolina (lisoPC) ha forma di cono invertito e rimane confinata nel foglietto esterno della membrana, gli acidi grassi hanno forma a cono, ma si ripartiscono velocemente su entrambe i foglietti. Questa alterazione della composizione lipidica della membrana plasmatica ne provoca una deformazione che rende più facile il processo di fusione con le vescicole sinaptiche, cioè facilita la transizione tra intermedio di emifusione e poro aperto; per le stesse ragioni invece inibisce l'endocitosi, necessaria per il recupero delle vescicole stesse e il mantenimento della funzionalità della sinapsi.

Analoghi risultati di blocco della neurotrasmissione sono stati ottenuti testando lisofosfolipidi con diverse teste polari; in particolare, lisolipidi dotati di carica negativa, in presenza di alte concentrazioni di magnesio, sono in grado di provocare un andamento trifasico della paralisi (iniziale depressione,

facilitazione, diminuzione progressiva della contrazione muscolare) ritenuto tipico delle SPANs. Il fenomeno è reversibile mediante lavaggio con albumina, capace di complessare i lipidi e riequilibrare la situazione.

Le SPANs e i loro prodotti lipidici sono stati testati anche sulla giunzione neuromuscolare di *Drosophila melanogaster:* le tossine sono risultate inattive in questo modello, suggerendo la mancanza di recettori specifici, necessari alla loro azione. La miscela di lisoPC e acido oleico provoca invece un iniziale aumento del potenziale post-sinaptico eccitatorio, seguito dal blocco della neurotrasmissione, e un rigonfiamento dei bottoni sinaptici. Analogamente a quanto osservato sulla giunzione neuromuscolare di topo, il componente attivo è la lisoPC e il suo effetto sulla fusione delle vescicole sinaptiche sembra essere di carattere generale. Anche animali meno evoluti dei serpenti, come alcuni insetti ematofagi, contengono nella loro saliva concentrazioni significative di lisoPC, sufficienti a provocare nei modelli sperimentali effetti analoghi a quelli osservati con i lipidi sintetici. E' possibile che questi lipidi rappresentino una forma molto semplice di veleno ottenuto da fosfolipasi digestive, da cui si sono in seguito evolute le neurotossine.

L'effetto sulla fusione delle vescicole non è sufficiente a spiegare l'estensiva deplezione che si osserva dopo l'intossicazione. La prolungata produzione di lisolipidi e acidi grassi provoca un'alterazione della permeabilità della membrana allo ione calcio, che entra nella cellula principalmente dal mezzo esterno. Questo comporta una massiccia fusione delle vescicole sinaptiche, che coinvolge anche il pool di riserva, e alterazioni del metabolismo cellulare, soprattutto a carico dei mitocondri. Tossine coniugate con fluorofori sono visibili all'interno dei neuroni dopo tempi brevi di intossicazione e colocalizzano con i mitocondri. Su preparazioni di mitocondri isolati sono in grado di promuovere l'apertura del poro di transizione della permeabilità mitocondriale con un'efficienza proporzionale alla loro attività fosfolipasica; analoghi risultati si sono ottenuti con miscele di lisoPC e acidi grassi.

Blocco reversibile della neurotrasmissione, formazione di bulges nei neuroni e aumento dei livelli intracellulari di calcio sono prodotti, con cinetiche simili a quelle della lisoPC, anche da altre molecole anfipatiche di diversa struttura chimica, ma aventi una forma complessiva di cono invertito. Tra queste sono state testate miltefosina e perifosina, usate in terapia come agenti anti-tumorali,

e il lisolipide derivato dal PAF (Platelet Activated Factor).

La neurotossicità delle fosfolipasi di serpente deriva quindi da una elevata specificità e localizzazione dell'attività enzimatica; accanto a ciò è da considerare che la loro azione si esplica su un meccanismo che ha carattere più generale, cioè il ruolo dei lipidi nei processi di fusione delle membrane biologiche.

Abstract

The venom of many snakes contains presynaptic neurotoxins (**SPAN**, snake presynaptic PLA2 neurotoxin), which are able to block neurotransmission and induce muscular paralysis.

Structural motives are conserved across toxins, but quaternary structures vary considerably; we have therefore considered four toxins characterised by different structural complexity: Notexin (monomer), β-bungarotoxin (heterodimer), taipoxin (trimer) e textilotoxin (pentamer).

These toxins are endowed with PLA2 enzymatic activity; they hydrolyse the sn-2 ester bond of glycerophospholipids, thereby producing lysophospholipids (lysoPLs) and fatty acids.

It has been shown, by using equimolar mixtures of such lipids on isolated neuromuscular junction and on cultivated neurons, that they are able to reproduce the effects of toxins: the block of neurotransmission with alteration of the morphology of nerve terminals (depletion of synaptic vesicles (SVs), swelling, alteration of mitochondria) and the formation of bulges on neurites, characterised by accumulation of specific marker of SVs.

These findings have led to interpreting the toxin mechanism of action as driven by an imbalance between exocytosis and endocytosis, due to the different structural characteristics of the lipids being produced: the lysophosphatidylcholine (lysoPC) has an inverted-cone shape and remains in the external leaflet of the membrane; on the contrary, fatty acids have a cone shape and move fast to both leaflets of the membrane. Such alteration of the lipid composition of the membrane causes its deformation, which facilitates its fusion with the SVs (ie, it facilitates the transition between the hemifusion intermediate and the open pore) and at the same time inhibits endocytosis, which is necessary to recover empty vesicles and to maintain the functionality of the synapses.

Similar results, with regard to the block of neurotransmission, have been obtained when testing lysoPLs with different polar heads; in particular, lysoPLs with a negative charge are able, in presence of high magnesium concentrations,

to induce a triphasic pattern of paralysis (initial depression followed by increment of neurotransmitter release, and finally a progressive lowering of the muscular contraction), which is considered specific to SPANs. The phenomenon can be reversed by washing with albumin, which complexes lipids and restores the equilibrium.

SPANs and their lipid products have been tested also on the neuromuscular junction of *Drosophila melanogaster.* In this model, however, the toxins resulted inactive. This suggests that the specific receptors, which are necessary to their action, are missing. On the contrary, the mixture of lysoPC and oleic acid (OA) causes an initial increase of their excitatory postsynaptic potential, followed by the block of neurotransmission, and the bulging of synaptic buttons. Similar to what observed on the mouse neuromuscular junction, lysoPC is the active component; its effect on the fusion of SVs is more general than that of the toxins.

Significant amounts of lysoPC were detected in the saliva of hematophagous arthropods, which are at an earlier stage of the evolution process than snakes. When used in laboratory experiments, this is sufficient to cause a range of effects which are similar to those induced by the synthetic lipids. It is therefore conceivable that such lipids represent a very simple poison obtained from digestive phospholipases, from which neurotoxins could then have evolved.

The effect on the probability of SV fusion is not sufficient to explain the extensive depletion which is observed after intoxication. The prolonged production of lysoPLs and fatty acids causes an alteration of the membrane permeability to calcium, which enters into the cell mainly from the external medium. This effect induces a massive fusion of SVs, also involving the reserve pool, and the alteration of cell metabolism, notably for what concern the mitochondria. Toxins conjugated with fluorophores are visible inside the neurons a few minutes after intoxication, and they colocalise with mitochondria. When used on preparations of isolated mitochondria, such toxins are able to promote the opening of the permeability transition pore with an efficiency which is directly proportional to their phospholipasic activity; similar results were obtained with mixtures of lysoPC and fatty acids.

Other amphipathic molecules, with different chemical structure than lysoPC, but a broadly similar inverted-cone shape, are also able to induce a reversible block

of neurotransmission, the formation of bulges in the neurons and an increase in the intracellular calcium levels, with similar kinetics to lysoPC. In particular, miltefosine and perifosine (used in anti-tumoral therapies) as well as the lysolipid derived from PAF (Platelet Activated Factor) have already been tested.
The neurotoxicity of the snake phospholipases derives therefore from a high level of specificity and localisation of enzymatic activity; however, their mechanism of action is more general, as it is related to the general role of lipids in the biological membrane fusion process .

Introduction

Toxins and lipids

Many strategies have developed in nature to guarantee or improve the survival of species. Among them, a number of organisms have evolved the ability of synthesizing a type of molecules, called toxins, which are able to favor, in different ways, the producing organism.

Toxins found in nature are the product of long-term co-evolution processes involving species living within the same ecological niche. For this reason, such toxins have “learnt” to act on mechanisms that are fundamental for the host or the prey. Studying the molecular mechanisms which underpin the action of toxins is therefore very useful to better understand the physiological processes on which toxins act.

The work described in this thesis comes from the study on a group of neurotoxins referred as **SPANs** (snake presynaptic PLA2 neurotoxins), found in a number of venomous snakes. They act at presynaptic level, directly interfering with neurotransmitter release, and are endowed with type A2 phospholipase activity: this means that their substrates are lipidic molecules, in particular phospholipids that are hydrolyzed to lysophospholipids and fatty acids.

Lipids have been considered for a long time as passive elements, used by cells to constitutes bilayers. In fact, it is now usual to speak of “lipidomics”, in relation to the great number of different lipids found in eukaryotic cells: about 5% of their genes is invested in generating thousands of different lipids (van Meer *et al.*, 2008), and this class of molecules are increasingly recognised of key importance in cellular physiology.

Finally, it is important to point out that all the most poisonous toxins are neurotoxins. Given the essential role of the nervous system in animal physiology, even a minor biochemical modification of a few neurons may result in a profound modification of behaviour.

Against this background, the mode of action of SPANs and the effects induced by various lipidic molecules in neuronal models could be a very interesting fields to study.

The neuromuscular junction as a target for many toxins

The neuromuscular junction (NMJ), the most studied of all synapses, provides the link between myelinated motor nerves and skeletal muscle. As each myelinated motor axon reaches its target muscle it divides into 20–100 unmyelinated terminal fibres, each of which innervates a single muscle fibre. The combination of the terminal fibres from a motor axon and the muscle fibres they serve is called a motor unit.

NMJ is an integral part of an impressively efficient biological amplification system, which converts nerve action potentials into muscle contraction.

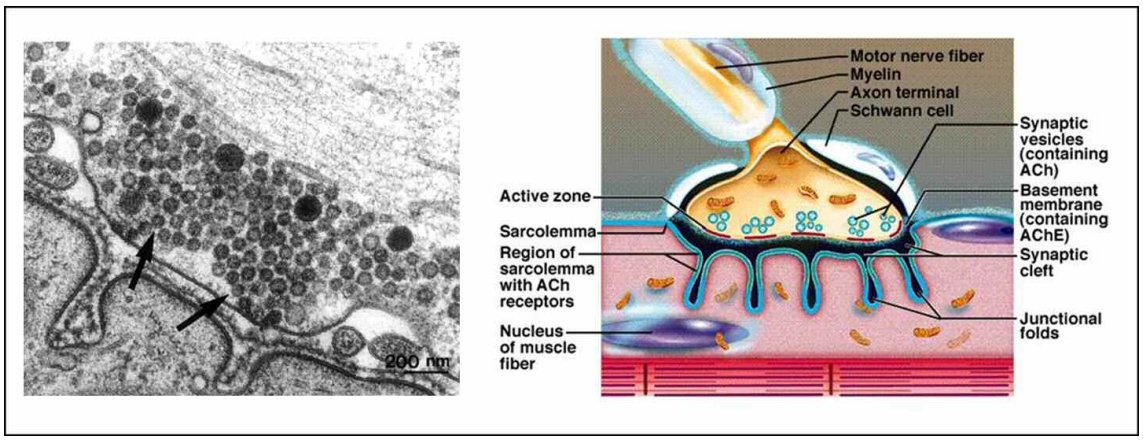

Figure 1: the neuromuscular junction. Electron microscopy (left) and schematic representation of its components (right).

This conversion is realized by a sequence of events that in its general schema is shared by almost all synapse, both in vertebrate or invertebrate. The action potential depolarisation causes the opening of voltage gated calcium channel, the increase of intracellular calcium concentration triggers the neurotransmitter release and finally, the binding of acetylcholine to its receptor starts the cascade of muscular events that lead to contraction. Many toxins produced by venomus animals act on various elements of this complex system, to cause the paralysis, or in some case the death, of the preys.

Two groups of toxins interfere directly with neurotransmitter release by exploiting their highly specific enzymatic activity at the presynaptic level: clostridial neurotoxins with metalloproteolytic activity and snake neurotoxins with phospholipase A_2 activity.

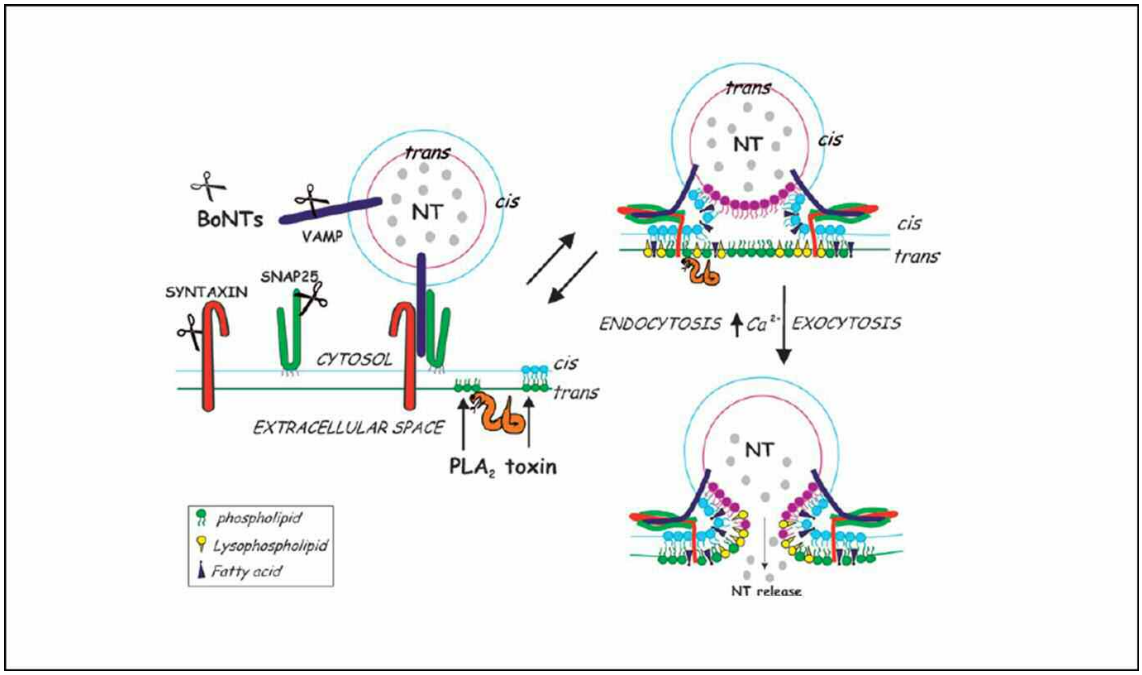

Figure 2: model of intoxication produced by clostridial neutoxins (BoNTs, scissors) and SPANs (snake). The first group cleaves SNARE proteins blocking the neuroexocytosis. The second group hydrolyses membrane phospholipids.

Despite the fundamental differences in the mode of action (Rossetto *et al.*, 2006, fig. 2), the study of all these toxins contribute to the understanding of the molecular steps of neurotransmission, and can open the possibility of their future clinical applications.

Lipids role on synaptic vesicle fusion

One of the crucial events in the synaptic transmission is the fusion of neurotransmitter containing vesicles with the membrane of the presynaptic terminal. The extremely spatial and temporal regulation of this process is fundamental for the nervous sistem.

Ultrastructural studies of synapses in different organisms have revealed the presence of highly specialized sites of the presynaptic nerve terminal, defined as “active zone” (AZ); conserved morphological features characterized these structures: the plasma membrane appears to be electron dense, suggesting its proteinaceous nature; the cytomatrix immediately internal to the plasma membrane is the site where synaptic vesicles dock; electron-dense projections, extending from the cytomatrix into the cytoplasm, are present and represent vesicles tethering sites; their morphology varies greatly among different types of synapses, but the primary function seems to be conserved).

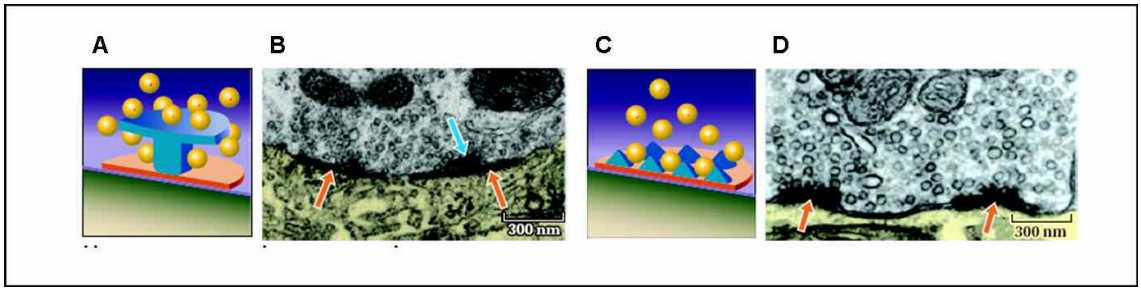

Figure 3: Electron micrographs and schematic representations of the active zone structures found in different synapses of various organisms. A and C are diagrams of the active zone structure in the synaptic terminal electron micrographs shown to their right. B: an NMJ terminal in Drosophila with a dense projection called a T bar (blue arrow). D: an excitatory synaptic terminal in human hippocampus with 2 active zones (red arrows). Adapted from Zhai and Bellen, 2004.

Moreover, the AZ is closely and precisely aligned with a postsynaptic density (PSD) area, and the extracellular space between the two membranes (synaptic cleft) is as narrow as 30 nm. These morphological characteristics suggest that AZs function as sites of synaptic vesicle exocytosis and neurotransmitter release (Dai *et al.*, 2007, Zhai & Bellen, 2004).

Many proteins are involved in different steps of neuroexocytosis; among these, the SNARE complex, formed by VAMP-synaptobrevin and the plasma membrane proteins syntaxin-1 and SNAP-25, has been thought to be the

driving force for bringing the membranes together, facilitating lipid bilayer mixing and subsequent membrane fusion; Munc and RIM proteins play a critical role in vescicle priming; synaptotagmyn-1 acts as a calcium sensor, with the ability to form quaternary complex with the SNARE complex, calcium and membrane phospholipids (Dai *et al.*, 2007).

The lipid composition of the membrane is also very important in this contest for two reasons: first, lipid domains can contribute to the specific localisation needed for some proteins, for example the clustering of calcium channel near the site of fusion; second, membrane fusion is catalyzed and regulated by proteins, but it is essentially lipidic in nature.

Protein-free bilayers of compositions that mimic those of biological membranes do not fuse; however, lipid bilayers can fuse in the absence of any proteins, depending on their lipid composition (Chernomordik & Kozlov, 2008).

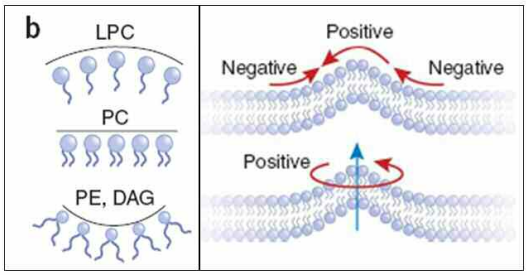

Figure 4: spontaneous curvature of different lipids. Membrane bending requires both negative than positive curvature

The impact of a given lipid on the formation of different fusion intermediates correlates with its effective spontaneous curvature — the curvature of a monolayer formed spontaneously by this lipid in the absence of constraints. The spontaneous curvature of a lipid is determined by its molecular structure and by lipid interactions within the monolayer (Chernomordik & Kozlov, 2003). Lipids such as lysophosphatidylcholine (lysoPC) and polyphosphoinositides tend to self-assemble into curved monolayers whose surfaces bulge in the direction of the polar heads. These curvatures are defined as positive and derive from lipid molecules that have the effective shape of an inverted cone.

In contrast, such lipids as unsaturated phosphatidylethanolamine, diacylglycerol and fatty acids tend to form monolayer with surfaces bulging in the direction of

the hydrocarbon chains. Hence, these lipids can be described as having a negative spontaneous curvature and cone-like effective shape.

Finally, lipids such as phosphatidylcholine tend to form almost flat monolayers with a slightly negative curvature and thus can be seen, in first approximation, as having the effective shape of a cylinder and a spontaneous curvature that is close to zero (fig. 4).

Membrane fusion reactions involve close contact between two lipid bilayers, followed by the local distortion of the individual bilayers, forming both positive than negative curvature (fig. 4). The most reliable intermediate in this process is the hemifusion structure, that represents a connection between outer leaflets of apposed membrane (referred as stalk), with distinct inner leaflets and without content mixing (Chernomordik & Kozlov, 2008).

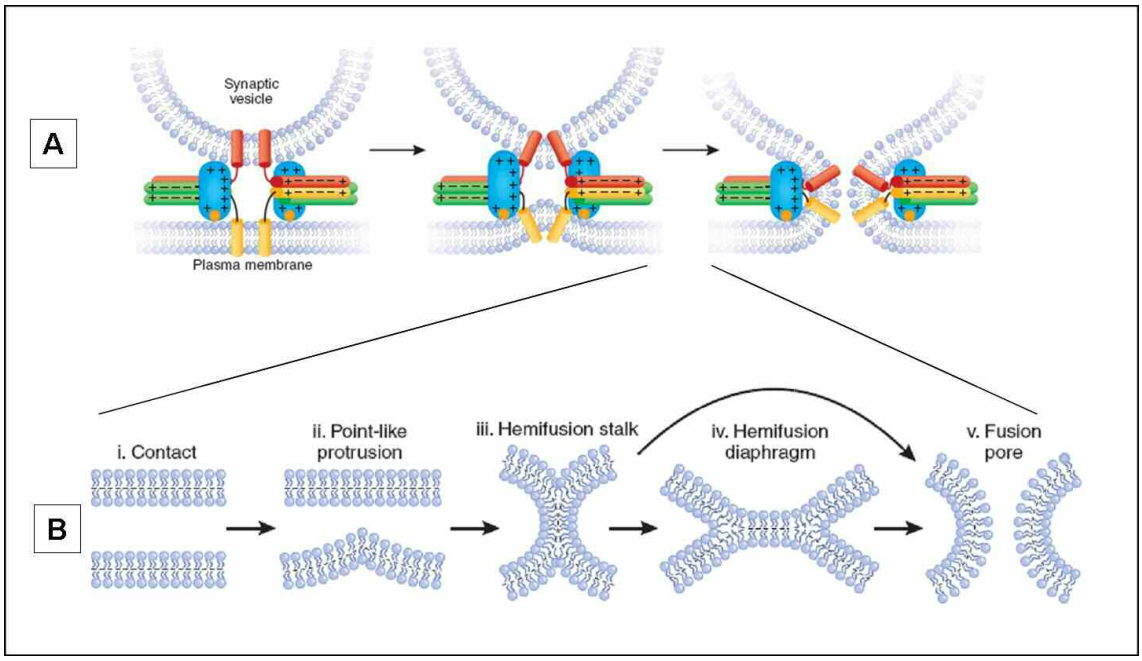

Figure 5: A) fusion of synaptic vesicle with the plasma membrane. This process is driven and controlled by many proteins. B) the formation of hemifusion intermediates during membrane fusion.

These structures are often transient, and can dissociates or give rise to a fusion pore. Most importantly for neuronal function, if a fraction of the synaptic vesicles are even transiently hemifused with the presynaptic membrane, they are at the

penultimate stage of exocytic fusion, awaiting fusion pore formation and poised to release transmitter very quickly. Thus, hemifusion can explain the extremely fast kinetics of neurotransmitter release (<100 µs after the intracellular calcium concentration rises) that characterize synaptic exocytosis (fig 5). The prediction that synaptic vesicles at the active zone make transient hemifusion intermediates also can explain the spontaneous release of neurotransmitter from vesicles (miniature postsynaptic currents) that is a hallmark of synaptic activity.

Toxins acting on lipids: the snake PLA2 family

Classification and structural organisation

Several snake venoms contain toxins with phospholipase A2 (PLA2) activity, and more than fifty of these presynaptic neurotoxins have been characterised so far. On the basis of their quaternary structures, they can be divided into four classes (Kini, 1997).

Class I comprises single chain toxins of molecular mass varying in the range of 13–15 kDa with seven disulphide bridges. This class includes, among others, notexin from *Notechis scutatus scutatus.*

Class II includes neurotoxic PLA2s composed of two non-covalently linked homologous subunits, at least one of which retains PLA2 activity.

Class III includes heterodimers composed of unrelated subunits, such as the most studied of PLA2 neurotoxin β-bungarotoxin. This toxin is manufactured by *Bungarus multicinctus* and it is composed of a 120 residue-long PLA2 subunit disulphide linked to a 7 kDa protein with a sequence and a structure very similar to that of the Kunitz-type trypsin inhibitor and to the three-foil sub-domain of the receptor binding domain of Tetanus neurotoxin.

Class IV comprises non-covalently associated oligomers of homologous subunits. This class includes taipoxin (from *Oxyranus scutellatus scutellatus*), which is made of a strongly basic PLA2 subunit of 120 residues, of a 120 residue-long non-toxic subunit and of a 135 residue-long glycoprotein subunit with eight disulphide bridges, which is non-toxic, but retains PLA2 activity. Textilotoxin is the most complex of these neurotoxins. It is produced by *Pseudonaja textilis textilis* and it is a 70 kDa pentamer of homologous subunits, all of them having PLA2 activity, two of which are disulphide bridged.

The high resolution structures of notexin and β-bungarotoxin have been determined (Westerlund *et al.*, 1992, Kwong *et al.*, 1995). They fold very similarly to pancreatic phospholipases with their characteristic six conserved disulphide bonds that greatly contribute to the stability and compactness of the molecule. The structure comprise the characteristic three α-helices with two β-strands (fig. 6).

Figure 6: A) molecular structure of notexin, a monomeric SPAN. B) the snakes that produce the neurotoxins used in this thesis.

A remarkable feature of these enzymes is a hydrophobic channel that accommodates the fatty acid chains of the phospholipid molecule and places the ester bond to be cleaved into the active site. The catalytic site is composed by four key residues: His48, Asp49, Tyr52 and Asp99. The histidine residue hydrogen-bonds the water molecule used for hydrolysis, whilst Asp49 coordinates and positions the Ca2+ ion which binds both the phosphate and the sn-2 carbonyl groups of the phospholipid molecule during the hydrolysis.

The structure contains also an interfacial binding site, which mediates the absorption of the enzyme onto the lipid-water interface; this process is strongly promoted by anionic anphipatic molecules such as fatty acids (Scott,1997).

SPANs are major components of the venom of four families of venomous snakes (*Crotalidae*, *Elapidae*, *Hydrophiidae* and *Viperidae*). These neurotoxins play a major role in envenomation of the prey (Harris 1997) by causing a persistent blockade of neurotransmitter release from nerve terminals (Kini 1997; Schiavo *et al.*, 2000; Rossetto & Montecucco, 2008). In fact, independently on the anatomical site of biting, patients are reported to have ptosis, diplopia, ophthalmoplegia, difficulty in swallowing, respiratory paralysis, abdominal pain and autonomic symptoms. Intraperitoneal injection of these toxins in animals causes death by paralysis of respiratory muscles.

SPANs neurotoxicity and enzymatic activity

The reaction catalysed by SPANs is the hydrolysis of the sn-2 ester bond of 1,2-diacyl-3-sn-phosphoglycerides, producing fatty acids and lysophospholipids; their specificity reside on the position of the bond hydrolysed: the analogue ester bond in position 1 was not a substrate for these enzymes, whereas they recognise various molecules with different structure of the polar head and length of fatty acids (fig. 7).

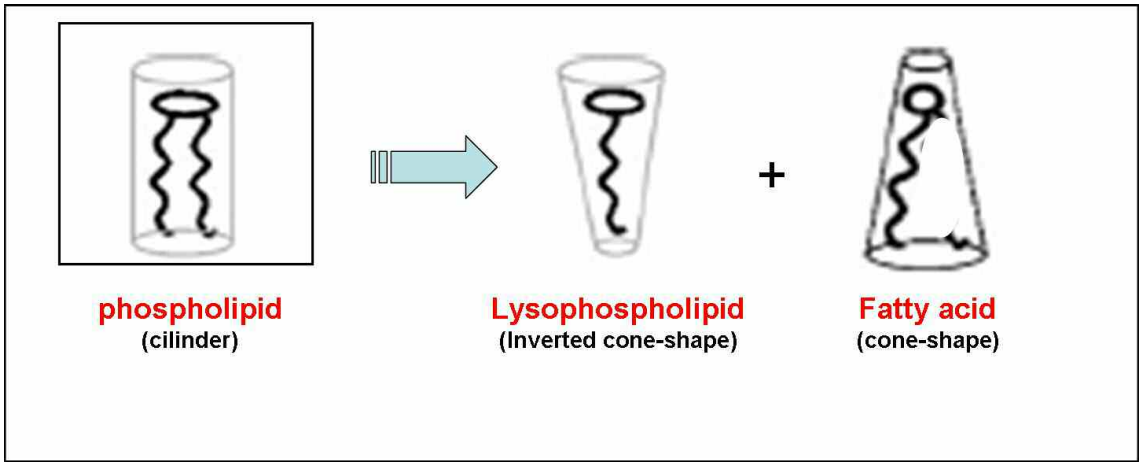

Figure 7: the PLA2 enzymatic activity of SPANs convert phospholipids in lysophospholipids and fatty acids.

The role of PLA2 activity in the intoxication of SPANs has been discussed at length in literature. For this class of toxins, there is no evidence of a direct correlation between the enzymatic activity, as measured *in vitro*, and the level of neurotoxicity (express as mouse LD_{50}) in the animal (Montecucco & Rossetto, 2000).

However, this can be explained by a number of factors (Rossetto & Montecucco, 2008). Firstly, the *in vivo* effect is the result of a sequence of events (distribution of the molecule in the organism, stability at degradation, possible binding to receptors). The enzymatic activity represents only the last step of this sequence and its contribution is not assessed separately in the animal model. Secondly, the comparison is made across PLA2 values obtained using different techniques (for instance with regard to the substrates used, or to

the measurement methods, with different level of sensitivity and accuracy). Such differences can affect substantially the PLA2 value observed, which makes it difficult to compare across such values. Finally, one should also consider that different batches of purified toxins may show some differences, deriving from the purification process itself.

Four SPANs of different structural complexity and relative toxicity were used in the work described in this thesis: the single-chain notexin (Ntx, 14 kD, from *Notechis scutatus*), the two-subunit β-bungarotoxin (β-Btx, 21 kD, from *Bungarus multicinctus*), the three-subunit taipoxin (Tpx, 42 kD, from *Oxyuranus scutellatus*), and the five-subunit textilotoxin (Tetx, 72 kD, from *Pseudonaja textilis*), (fig. 6).

A more direct comparison between enzymatic activity and the neurotoxic effect can be made considering as a neurotoxicity index the paralysis time on the isolated neuromuscular junction (see below) and using for all toxins a unique method to determine the PLA2 activity *in vitro.* Good results were obtained with a colorimetric method based on the use of a synthetic thio-analogue of PC. Both these parameters are normally used to assess the potency of toxin batches, but their high cost limits the number of analyses.

	Batches 2007-8		Batches 2004-5	
TOXIN	**PLA2 ACT.** (µmol/min x mg)	**T 50%** 1 µg/ml	**PLA2 ACT.** (µmol/min x mg	**T 50%** 1 µg/ml
NTX	374	28’	170	57’
β-BTX	227	22’	150	126’
TPX	79	18’	-	-
TeTX	15	55’	14	71

Table 1: comparison between enzymatic activity (express as µmoles of substrate hydrolysed per minute per mg of toxin at 25°C) and the time needed to paralyzed isolated neuromuscular junction (express as T50%, minutes to achieve 50% of reduction of muscular twitch).

Such direct comparison shows a closer correlation (see Table. 1); for each toxin, changes in measured PLA2 activity induce similar changes to its efficiency of paralysis. More difficult is the comparison among different toxins: TPX and TeTX

show very efficient paralysis even with very low level of PLA2 activity. Given their complex structure, it is possible that other phenomena, such as the efficiency of binding to their receptors, are affecting the process (Montecucco & Rossetto, 2008).

It should be considered that the situation *in vitro*, where an high soluble substrate was used, was very different from that *in vivo*, where the toxin needs to reach lipid molecules inserted in an organised bilayer. Despite this limitation, this analysis was used also to compare the dependence of the hydrolysis rate of the four toxins from the concentration of divalent cations; normal buffer used in this assay contains 1 mM Ca^{++} and 1 mM Mg^{++}.

In the presence of micromolar level of Ca^{++} only β-BTX showed a clear slowing down of their enzymatic activity, suggesting a more strict dependence from Ca^{++} respect to notexin, taipoxin and textilotoxin, whose activity was unaffected by this condition. Any of the toxins tested showed instead modification in presence of higher concentration of Mg^{++} (up to 6 mM).

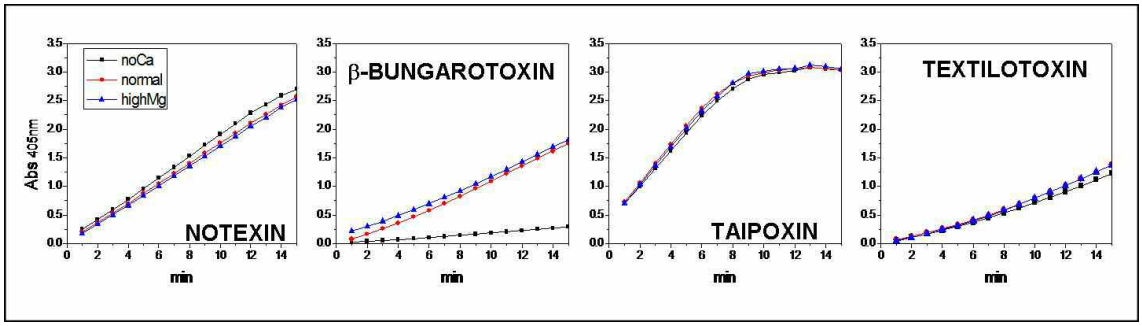

Figure 8: graphs showing the progressive increment in absorbance at 409 nm caused by PLA2 activity of indicated toxin using diheptanolyl thio-PC as a substrate. Red traces: standard buffer; black traces: standard buffer without added calcium and without EGTA; blue traces: standard buffer with 6 mM Mg^{++}.

A direct measure of SPANs' PLA2 activity *in vivo* can be obtained from the determination of hydrolysis products in toxin-sensitive cellular models. Such measure entails significant technical difficulties, due to the complexity of samples and to the low concentrations of lipids to detect. It is nevertheless possible by using mass spectrometry.

Cerebellar granule cells were treated with SPANs and their lipid composition

was determined by using this tecnique. The major hydrolytic substrate was phosphatidylcholine, the main phospholipid of the outer leaflet of the plasma membrane. SPAN hydrolysis generated several lysophosphatidylcholines (lysoPC), including myristoyl lysophosphatidylcholine (mLysoPC), and FA. SPANs were not selective for a particular FA species (such as arachidonic acid) and released mainly oleic acid (OA), the most abundant FA of these cells. Small percentage of lysoPE and lysoPS was also detected, suggesting the possibilty that SPANs acts both outside than inside the cell.

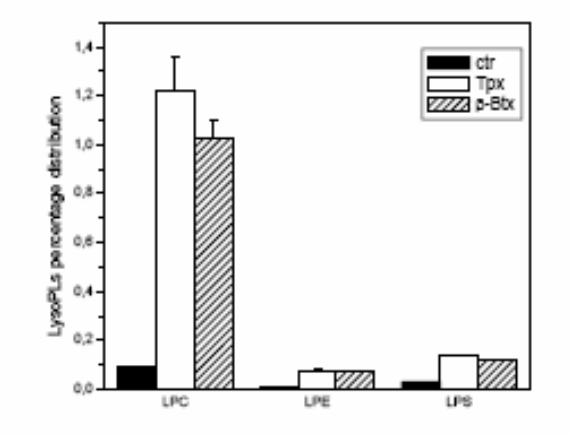

Figure 9: lysolipids contents in cerebellar granule cells treated with SPAN

This results demonstrate for the first time that SPANs really exert their enzymatic activity on cells, and their principal products are lysophosphatidylcholine and fatty acid.

Features of paralysis induced by SPANs in NMJ models

Frog, rat, mouse and drosophila nerve–muscle preparations are widely used in literature as a good model to work on isolated NMJ; they allow one to study the toxin effects on their natural target, bypassing the complex pharmacokinetic of proteins injected in animals.

Many observations on mechanism of SPANs intoxication derive from these models (Rossetto and Montecucco 2008): the toxic effects can be neutralized by anti-toxin antibodies or by washing, only if performed within a short time period (few minutes) after toxin addition; no competition among the different neurotoxins was evidenced; the time course of paralysis is greatly shortened by nerve stimulation. All these data strongly suggested that the first step in SPANs intoxication is the binding to a cellular receptor, probably distinct for each toxin. To date, the molecular identity of this receptor is not known, except for β-bungarotoxin whose smaller subunit binds to K^+ channels of the presynaptic membrane of peripheral nerves (Awan & Dolly, 1991).

Other fundamental observations derive from electron microscopy studies. NMJs intoxicated by SPANs show enlarged axon terminals with large depletion of synaptic vesicles, including those close to the membrane (ready to release pool) and those occupying a more internal position (reserve pool). There are several clathrin-coated Ω-shaped plasma membrane invaginations, also in areas not facing the muscle membrane foldings. Mitochondria are swollen with altered cristae so much as to appear in some cases as large vacuoles (Cull-Candy *et al.*, 1976; Dixon and Harris 1999; Gopalakrishnakone and Hawgood 1984; Harris et al. 2000; Prasarnpun et al. 2004). Even at this late stage of SPANs intoxication, no damage of muscles, fibroblasts and Schwann cells is noticeable. Observations made at later stages (several hours after treatment) both in frog and rat muscles show that the nerve terminal of the motor neuron axon virtually disappears from the endplate. This is accompanied by protrusions of Schwann cells establishing extensive contacts with the muscle fiber, similarly to what happens after several days of mechanical denervation.

The mouse phrenic nerve-emidiaphragm model

This experimental model is based on the isolation of the mouse diaphragm together with the phrenic nerve by which it is controlled. Using apposite electrodes it is possible to generate on the nerve repeated action potentials that cause the neurotransmitter release and the muscle contraction: the system represents a complete and perfectly functional NMJ, that when kept in optimal conditions in term of temperature, oxygen, glucose, and stimulation frequency, is able to work for more than 10 hours (fig. 10).

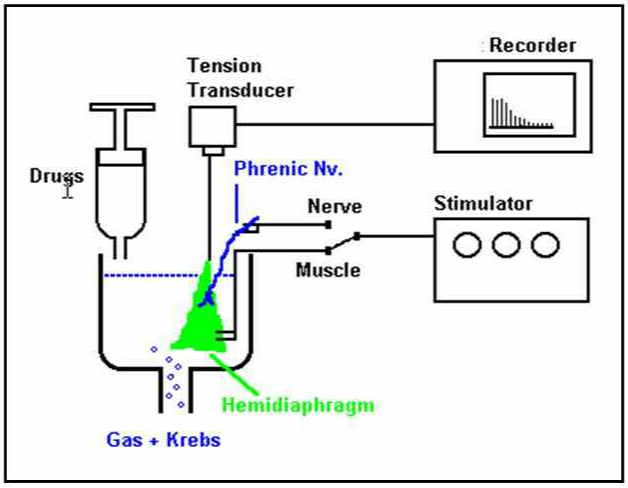

Figure 10: schematic representation of the experimental set-up used for experiments with mouse phrenic nerve-hemydiaphragm preparations.

Upon addition of the toxin into the oxygenated bathing medium, it is possible to monitor the alteration of muscular contraction that they cause which, in this case, is an indirect read-out of neurotransmitter release. A final concentration of toxin ranging from 0,5 to 3 µg/ml causes a progressive decline of the muscular twitch, with time needed for complete paralysis of about 100-200 minutes, depending which toxin is used (Rigoni, 2004). To compare different experiments, it is useful to normalize the muscular twitch to its initial maximum value and to express the paralysis time as T 50%, i.e. the time needed to achieve 50% of reduction of muscular twitch; the measure of total paralysis time could be affected by bigger errors.

A widely used protocol to test these toxins at NMJ consist in lowering the initial

muscular twitch with the addition of magnesium (or reducing calcium levels in the buffer); the purpose of this experimental protocol is to reveal also possible increments in the neurotransmitter release. In this condition, SPANs show a peculiar profile of paralysis, represented by a triphasic curve (fig 11A): 1) a brief initial phase of weak inhibition of Ach release, lasting few minutes; 2) a more prolonged phase of facilitate neurotransmitter release; 3) a third phase of progressive decline of neurotransmission. Phase 1 and 2 are absent with some toxins such as notexin; other presynaptic neurotoxins, for example BoNTs, give in high [Mg^{2+}] a profile of paralysis completely equivalent to that obtained in physiological buffer, suggesting that the phenomena observed with SPANs is a peculiarity of the mechanism of action of this toxins.

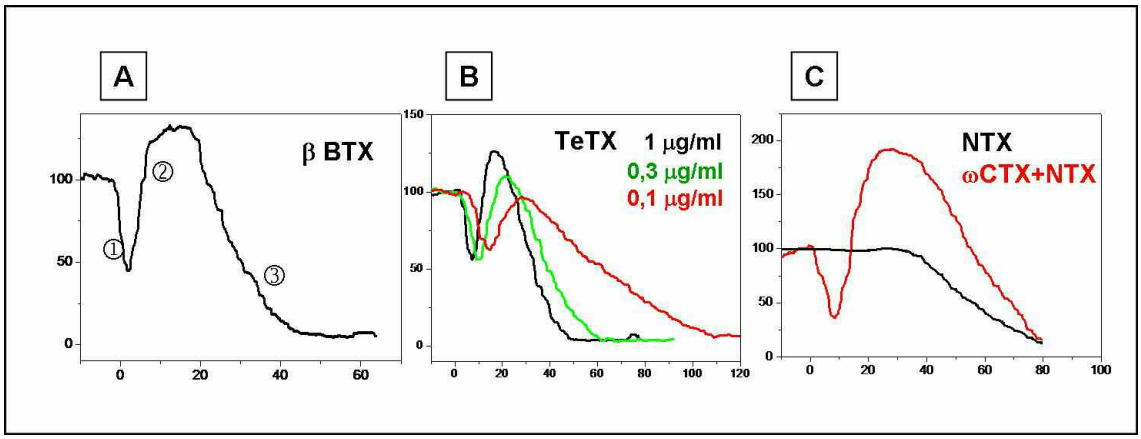

Figure 11:relative muscular twitch of mouse hemydiaphragm intoxicated with various SPANs added at time 0. See the text for details.

The molecular events underlying phase 1 and 2, (only present in high [Mg^{2+}]), are not known, but there are some data to consider about this point:

a) the variations with the dose are different for the two phases: as shown in fig. 11B for textilotoxin, the initial depression phase is essentially independent from toxin concentration, whereas the facilitation phase is dose dependent. These data are in good agreement with previous data from the literature (Rossetto & Montecucco, 2008)

b) the in vitro PLA2 activity of toxins, measured using a synthetic substrate (dyepthanoyl thio-PC), was tested at various [Mg^{2+}], but any significant difference was found respect to the physiological magnesium level.

c) a great increment of both phase 1 and 2 is observed when the muscular

twitch is reduced with ω-conotoxin MVII C, a blocker of P/Q type calcium channel, before adding SPANs. In this condition also notexin shows a triphasic profile of paralysis (fig. 11C). If the conotoxin is added after SPANs, the profile of paralysis is unaltered

Equivalent effect of toxins and their lipidic products

One of the first hypothesis about the mechanism of action of SPANs was that they act via the hydrolysis of phospholipids of the plasma membrane, and a long list of studies were dedicated to test this possibility. The experimental approach was indirect: it try to determine the consequences on neurotoxicity of inactivating the enzymatic activity. Chemical modifications of PLA2 specific residues or use of divalent cations which do not support the PLA2 catalytic activity were used in these studies; more recently this issue was approached by site-directed mutagenesis (Chioato *et al.*, 2007; Petan *et al.*, 2007). In general, the reduction or abolition of PLA2 activity of neurotoxins was correlated to a varying extent with loss of toxicity, but no conclusive evidence about the involvement of the PLA2 activity in toxicity was obtained.

A different and more direct approach was developed (Rigoni *et al.*, 2005) using SPANs hydrolysis product themselves. Using mass spectrometry, the production of lysoPC and fatty acids was measured in neuronal cells treated with toxins (see fig). Moreover, the same tecnique was employed to asses what happened in cells incubated with an equimolar mixture of myristoil lysoPC (mLysoPC) and oleic acid (OA), very similar to that generates by SPANs.

The incubation of cerebellar neurons with mLysoPC+OA (30 mM each) led to the incorporation of 6.3 nmol of mLysoPC/10^5 cells, compared with 2.3 nmol/10^5 cells treated with 6 nM taipoxin. The mixture did not cause acylation, because the 14:0 to 16:0 ratio in PC did not increase. Despite the great difference between the two treatments, the values of lysoPC associated with neurons in the two cases were closely comparable; accordingly to these data, the mixture mLysoPC+OA was then used in most experiments on both NMJ and neuronal cells.

Mouse neuromuscular junction

Fig. 12 shows that the addition of these lipids in the bathing medium, containing a physiological solution, causes a progressive paralysis of the mouse nerve hemidiaphragm which is superimposable to the trace obtained with a typical SPAN.

The concentration used was not toxic for the muscle, since direct muscle stimulation elicited full contraction also when the neurotransmission is completely abolished.

Of the two products of phosphatidylcholine hydrolysis by PLA2, lysoPC alone is capable of inducing muscle paralysis, though at higher doses, whilst OA alone is ineffective until it reaches concentrations that are toxic to the muscle. However, OA clearly potentiates the effect of lysoPC.

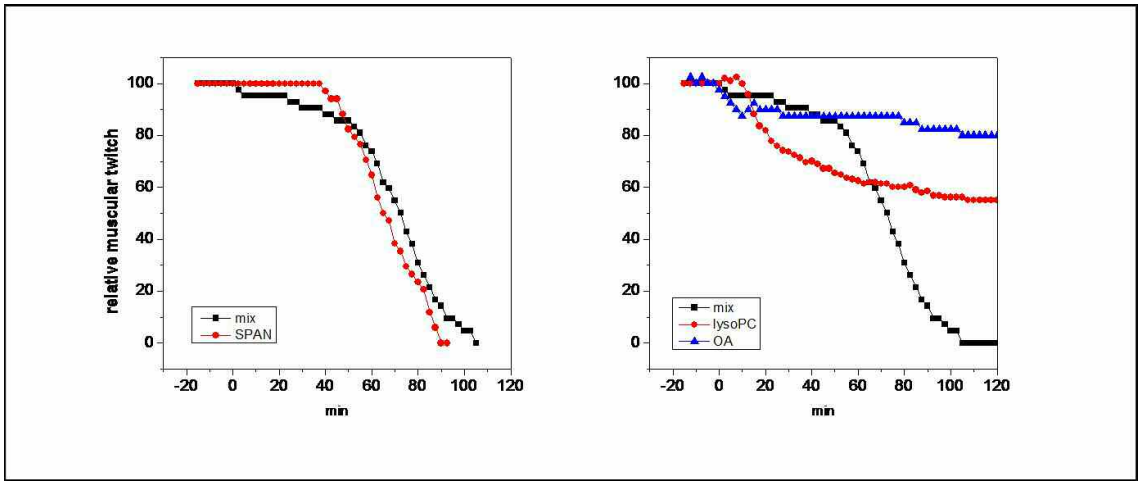

Figure 12: comparison of relative muscular twitch of mouse hemydiaphragm treated with SPANs or lipids, added at time 0. See the text for details

The comparison was made also at the ultrastructural level: electron mycroscopy of mouse NMJ paralyzed by the mixture show remarkable alteration of the presynaptic moiety with enlargement of the nerve terminal, depletion of synaptic vesicle and swollen mitochondria, as previously described for SPANs. On the contrary, the muscular portion is perfectly conserved, as observed by functional tests.

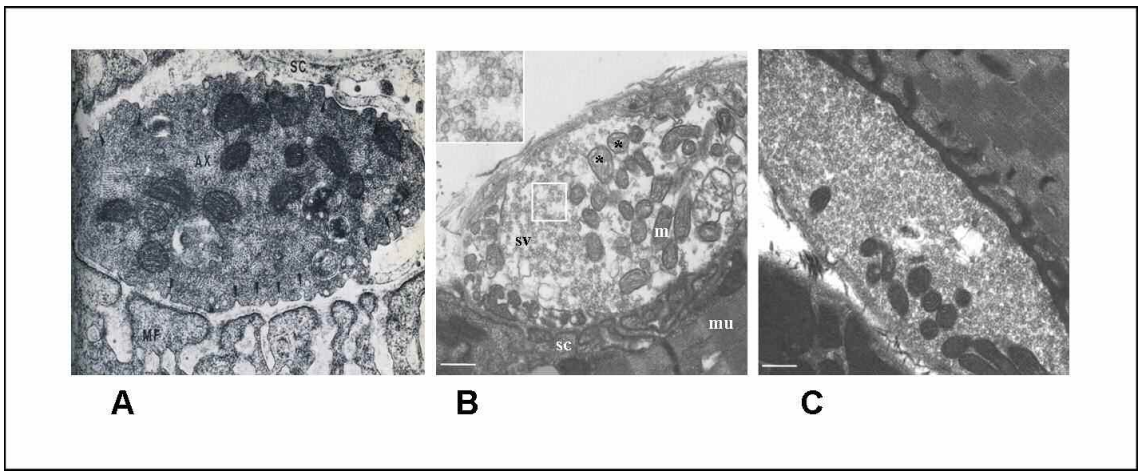

Figure 13: A) electron microscopy of taipoxin treated mouse NMJ; B) equimolar mixture of myrstoilLysoPC and OA; C) control

LysoPC esterified with FAs of different length and saturation were also tested, obtaining similar profile of paralysis, but different potency (table 2). This data well correlates with the critical micellar concentration of each lipid, indicating that the more water-soluble lysoPC equilibrates more rapidly into the membrane and acts faster; it is also possible that the shorter lysoPL causes a higher constraint on the membrane curvature.

lipid	CMC	Relative T50%
LPC-MYRISTOYL C 14:0	0.07 mM	1
LPC-OLEOYL C 18:1	0.0004 mM	2,2±0,5
LPC-PALMITOYL C 16:0	0.007 mM	3,2±1,3
LPC-STEAROYL C 18:0	≈Ins.	8,5±0,6

Table 2: CMC: critical micellar concentration; the T50% values are expressed relative to that of myristoilLysoPC

If lipids are the biochemical mediator of the action of SPANs, the contemporary

presence of exogenous lipids and toxins is expected to produce a synergistic effect; indeed, when textilotoxin and mLysoPC+OA were present at the same time (1.5 nM and 50 mM, respectively), the $T_{50\%}$ is four-fold shorter than that of textilotoxin. Another interesting observation concerns the activity on NMJ of non neurotoxic PLA2 enzymes. Pancreatic PLA2 (at a concentration matching the activity of SPANs in the same experiment) did paralyze the NMJ, but with a $T_{50\%}$ three times as long , whereas phospholipase from bee venom are not able to induce muscular paralysis in mouse hemidiaphragm (not shown). These results are in good agreement with the hypothesis that the toxicity of SPANs derives from a strictly localised hydrolytic activity; other enzymes, probably because of a reduced membrane interaction, are very less effective.

Neuronal cell models

In cultured neurons SPANs induced a characteristic swelling (Rigoni *et al.*, 2004, Bonanomi *et al.*, 2005) with depletion of synaptic vesicles, release of glutamate and FM1-43, and surface exposure of the intralumenal portion of the synaptic vesicle protein synaptotagmin I (SytI).

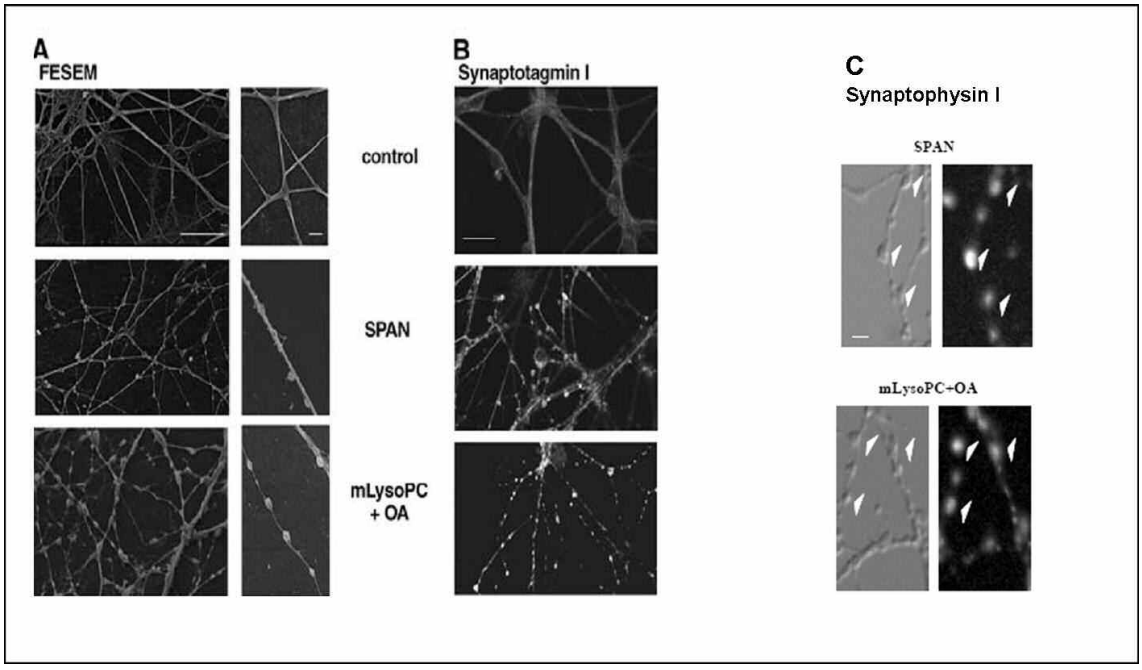

Figure 14:comparison of SPANs and their lipidic products on cerebellar granule cells by electron microscopy (A) and immunocytochemistry with indicated antibodies.

Neuronal cells were therefore incubated with the mixture mLysoPC+OA, used in NMJ experiments. In cerebellar granule cells these lipids induced bulges (fig 14A) that were strongly stained by an antibody specific for the lumenal domain of SytI in the absence of membrane permeabilization, indicating a persistent surface exposure of the inside of synaptic vesicles (fig. 14B). Control experiments showed no labeling with an antibody specific for a cytosolic SytI epitope, indicating that the mLysoPC+OA mixture did not permeabilize the neuronal membrane. Moreover, a staining of lipids treated cells with an antibody specific for synaptophysin I, a marker of SV, clearly indicated that this protein is enriched in bulges (fig 14C).
All these data allow to interpret bulges as sites of enhanced vesicles fusion, where the lack of a balanced endocytosis results in a membrane swelling.

How can the biological action of SPANs and their hydrolysis products at nerve terminal be rationalised? Two aspects need to be considered: first, the molecular properties of lysoPLs and FAs with respect to those of phospholipids and second, the molecular mechanism of synaptic vesicle fusion.
Phospholipids have a rather cylindrical shape with a balance between the hydrophilic head group and the hydrophobic fatty acid chains, as to be compatible with the formation of a bilayer membrane structure. LysoPLs have an inverted cone shape and a lower hydrophobic portion with respect to phospholipids; they spontaneously form spherical micelles in polar solvents. When they are comprised within bilayer biological membranes, they induce a positive curvature of the membrane layer where they are located; in the case of the toxins, or of the lipids added to cells, this is the outer monolayer of the plasma membrane. Long-chain FAs are cone-shaped and hydrophobic, and at variance with lysoPLs, they have a high mobility such that they can rapidly move from one membrane layer to the other. This high flip-flop rate allows their rapid equilibration in the two layers of biological membranes.
The resultant membrane organisation is fusogenic: the energy barrier needed to fusion is lowered; this modification has a great impact on nerve teminal, where the ready-to-release pool of SVs is suggested to be already hemifused with the presynaptic membrane: this would account for the ultra-fast event of neuroexocytosis that takes place within few hundreds of microseconds from the

entry of calcium (Zimmerberg & Chernomordik, 2005). For the same reason, the membrane configuration induced by the SPAN hydrolytic action inhibits membrane fission, which is the reverse of the membrane fusion, and is essential for the recycling of the empty SVs.

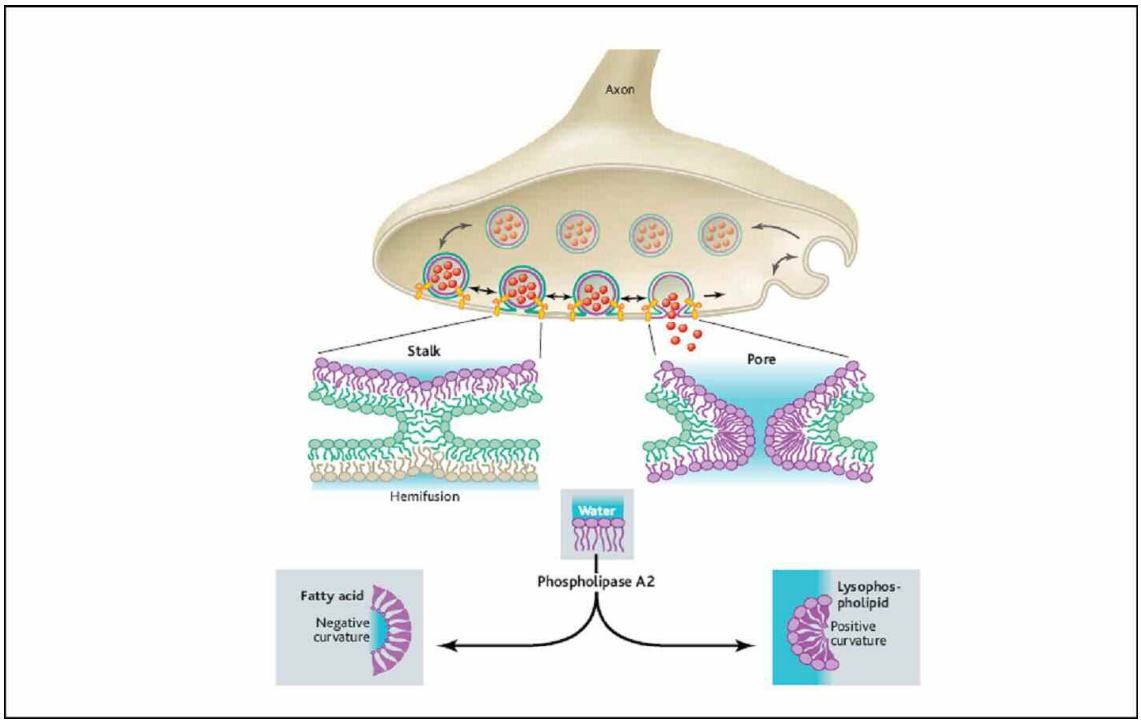

Figure 15: Lipids alter membrane bending at the synapse to control vesicle fusion and synaptic activity. Membrane fusion between a synaptic vesicle containing neurotransmitter molecules (red) and the plasma membrane of a presynaptic neuron is hypothesized to proceed through the formation of a hemifusion intermediate followed by the formation and expansion of a fusion pore. Lipid mixing between the inner (purple) and outer (green) leaflets of the vesicle membrane and plasma membrane (tan) at early fusion stages is likely restricted by the proteins (yellow ribbons) surrounding the fusion site.The connection between contacting leaflets of two bilayers (the stalk) is favored by lipids that support negative leaflet curvature. In contrast, the curvature of the edge of the fusion pore,formed by distal bilayer leaflets brought together by hemifusion, is favored by positive curvature lipids. Phospholipase A2 cleaves lipids that form flat monolayers into lyphospholipids (positive curvature) and fatty acids (negative curvature).

Other inverted-cone shaped lipids

On the basis of the findings obtained with lysoPC, the effects on neurons of other molecules of similar shape, but of different chemical nature and biological properties was tested, in order to determine if the effect is a general one and if it can be attributed mainly to the shape of the molecule rather than to the presence of a particular phospholipid head group.

The first group of lipids tested comprised natural glycerolysophospholipids with different polar head, compared on NMJ model.

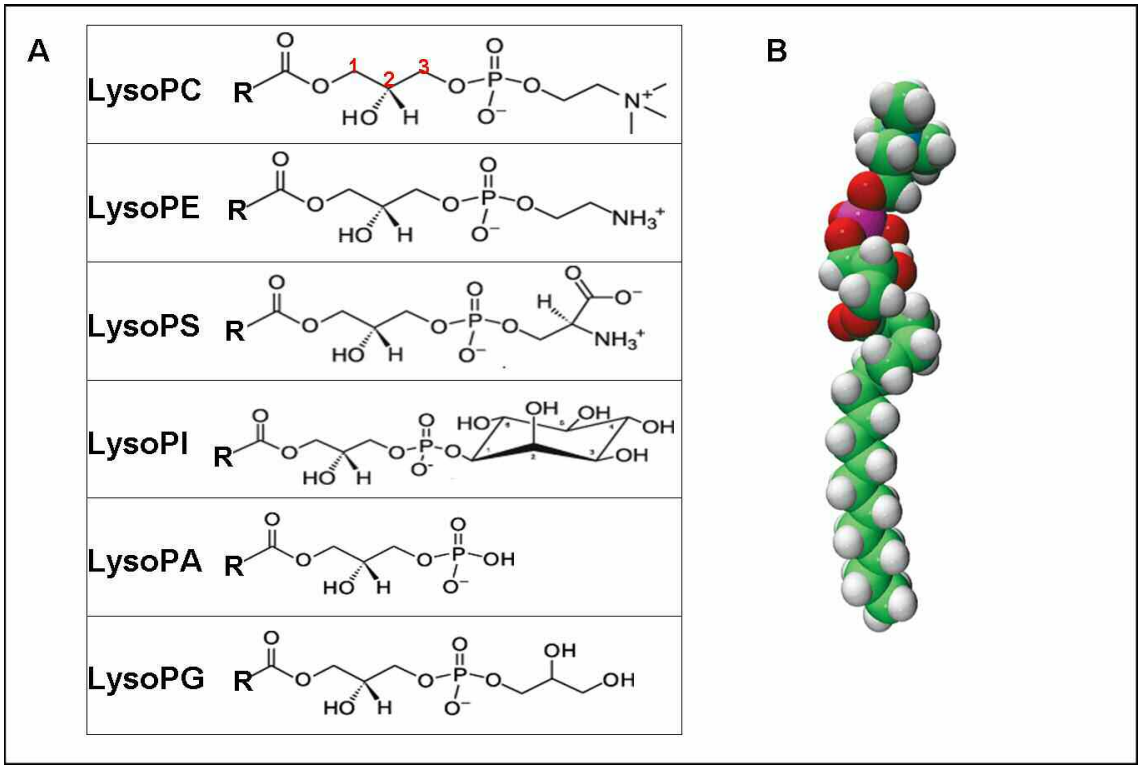

Figure 16: A) chemical structure of the polar head of the lysoPLs used in this thesis. Numbers in red on lysoPC structure indicate the three carbon atoms of glycerol backbone; R: fatty acid in position 1. B) model of lysoPC.

The effects of other inverted-cone shaped molecule (miltefosine, perifosine, and the lyso derivatives of the platelet-activating factor, lysoPAF) was then analyzed and compared to lysoPC. Miltefosine and perifosine are alkylphosphocholines

developed from alkylphospholipids, in which the glycerol backbone is lacking. They have a strong anti-proliferative effect on many cellular models, and are used as anticancer drugs but they are membrane–targeted and do not interact with DNA (Floryk & Thompson, 2008, Vink *et al.*, 2007).

LysoPAF is a natural lipid produced in cells by a regulated $cPLA_2$ that acts on alkylphospholipids; it is an intermediate in one of the synthesis pathways of platelet activating factor, but the lack of the acetyl group makes it unable to bind the PAF receptor (Prescott et al., 2000). The main difference from LysoPC is the ether bond that links the hydrocarbon chain with the polar head (fig.17).

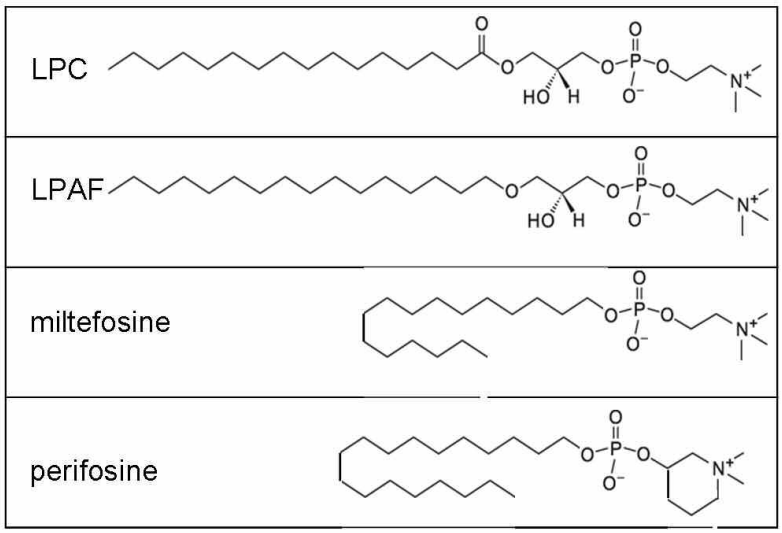

Figure 17:) chemical structure of the alkil lipids choosed for this work.

Materials and methods

Materials

Taipoxin and textilotoxin were purchased from Venom Supplies (Tanunda, South Australia); β-BTx was from Sigma (Saint Louis, MS, USA). Purity was checked by sodium-dodecyl-sulfate polyacrylamide-gel electrophoresis (SDS-PAGE). Bovine serum albumin (BSA) was from Roche (Indianapolis, IN, USA). Lysophosphatidylcholine (1-myristoyl-2-hidroxy-sn-glycero-3-phosphocholine and 1-oleoyl-2-hidroxy-sn-glycero-3-phosphocholine) and oleic acid (sodium salt) were purchased from Sigma. Lysophosphatidylethanolamine (1-myristoyl-2-hydroxy-sn-glycero-3-phosphoethanolamine), lysophosphatidylserine (1-oleoyl-2-hydroxy-sn-glycero-3-phosphoserine), lysophosphatidylglycerol (1-myristoyl-2-hydroxy-sn-glycero-3-[phospho-rac-(1-glycerol)] (sodium salt), and lysophosphatidyc acid (1-oleoyl-2-hydroxy-sn-glycero-3-phosphate (sodium salt) were obtained from Avanti Polar lipids (Alabaster, AL, USA).
LysoPAF (1-O-Palmitoyl-sn-glycero-3-phosphocholine) were obtained from Sigma. Miltefosine (1-hexadecylphosphorylcholine) and perifosine were from Cayman Chemical Company (Ann Arbor, MI,USA). Fura2-AM and Pluronic acid were from Molecular Probes (Eugene, OR); all other chemicals were of analytical grade (Sigma).

Lipids preparation

Suitable amounts of lysophospholipds and lysoPAF were dissolved in small volumes of $CHCl_3$:CH_3OH (3:1, v/v), dried to a thin film under a gentle nitrogen flow and vacuum pumped for at least 2 h to remove residual traces of organic solvents. The dried lipid film was suspended in buffer L (Hepes-Na 10 mM, pH 7.4, NaCl 150 mM) at a final concentration of 5 mM, extensively vortexed and then ultrasonically dispersed in a bath sonicator at 37°- 40°C, until optical clarity was achieved. Miltefosine and perifosine and oleic acid were suspended directly

in buffer L (final concentration 5 mM), vortexed and ultrasonically dispersed with the same procedure, at room temperature.

Mouse phrenic nerve-hemidiaphragm preparation

All experimental procedures were carried out in accordance to the European Communities Council Directive n° 86/609/EEC. Mouse phrenic nerve hemidiaphragms were isolated from CD-1 mice weighing about 20-30 g following established procedures (Bulbring E., 1946) and mounted in 20 ml oxygenated (95% O_2, 5% CO_2) solution (139 mM NaCl, 12 mM $NaHCO_3$, 4 mM KCl, 2 mM $CaCl_2$, 1 mM $MgCl_2$, 1 mM KH_2PO_4 and 11 mM glucose, pH 7.4). Two innervated hemidiaphragm preparations were isolated from each animal.
The phrenic nerve was stimulated via two ring platinum electrodes with supramaximal stimuli of 10 V amplitude and 0.1 millisecond pulse duration, with a frequency of 0.1 Hz (Stimulator 6002, Harvard Apparatus, Massachusetts, USA). Muscle contraction was monitored with an isometric transducer (Harvard Apparatus); data were recorded via a NI DAQCard-6062E and analyzed by a LabView-based computer program (National Instruments, Austin, Texas, USA); the twitch amplitude was calculated as a difference from basal muscular tension and the mean of peak value measured after stimulation.
Muscles were stretched to the optimal length for twitch tension and the muscle twitch allowed to stabilize for at least 20 min at 37°C. In control experiments the amplitude of muscle contraction under this type of stimulation was constant for at least 8 hours. Aliquots of a 0.5 M solution of $MgCl_2$ were added to the bath to obtain a twitch reduction from 45 to 55% of initial stabilized twitch. Muscles were equilibrated for further 15-20 min; the mean twitch value measured during the 5-10 min before addition of lipids was taken as 100% in order to normalize the experiments.

Cell cultures

Primary rat spinal motor neurons (SCMNs) were isolated from Sprague-Dawley

(embryonic day 14) rat embryos and cultured following previously described protocols (Arce et al., 1999; Bohnert & Schiavo, 2005). All experiments were performed using SCMNs differentiated for 5–8 days in vitro.

NSC34 is an immortalized motor neurone cell line, (Cashman et al., 1992, kindly provided by Dr A. Poletti, University of Milan, Italy). These cells were routinely maintained in Dulbecco's modified Eagle's medium (DMEM) with sodium pyruvate, supplemented with 10% fetal bovine serum (FBS, Euroclone, Pavia, Italy), 100 UI/mL of gentamicin (Sigma) and grown at 37°C in 5% CO_2 in 25 cm^2 flasks, changing the medium every 72 h. The cells were detached from the plate by mechanical dissociation in culture medium.

For microscopy, NSC34 were plated on 24 mm coverslips (2-3x10^4 cells/well) coated with poly-L-lysine (Sigma) for time lapse experiment, or matrigel (BD Biosciences, NJ, USA) for calcium imaging. Differentiation was induced by lowering the serum content to 5% and by addition of retinoic acid at a final concentration of 10 µM and well differentiated cells with long neuritis were obtained after 5-6 days..For viability assay, cells were plated on 96 well plate coated with poly-L-lysine, 5000 cells/well in 100 µl of medium and used 3 days after plating.

HeLa, SH-SY5Y and Neuro2A cells (from ATCC, American Type Culture Collection, Manassas, VA, USA) were cultured in DMEM with 10% FBS and detached from the plate by trypsin. For viability assay, cells were plated on 96 well plate (15,000 cells/well, 5,000 cells/well, and 10,000 cells/well respectively) and used the day after plating.

Calcium imaging

Neurons grown on 24 mm coverslips were incubated in complete medium with 3µM Fura-2/AM and 0.02% pluronic acid for 20 min at 37°C and then washed. To prevent Fura-2 leakage and sequestration, 250 µM sulfinpyrazone was present throughout the loading procedure. After loading, cells were bathed in E4 medium (Extra-4 medium: 120 mM NaCl, 3 mM KCl, 2 mM $MgSO_4$, 2 mM $CaCl_2$, 10 mM glucose, and 10 mM HEPES, pH 7.4).

Coverslips were mounted on a thermostated chamber (Medical System Corp.), placed on the stage of an inverted epifluorescence microscope (Axiovert 100 TV; Zeiss), equipped for single cell fluorescence measurements and imaging analysis (Giacomello et al., 2005).
Samples were alternatively illuminated at 340 and 380 nm (every 10 s for 10–30 min after lipid exposure) through a 40x oil immersion objective (Zeiss, numerical aperture 1.30), exposure times of 200 ms. Control experiments in the same illumination condition do not show any increase in calcium concentration (not shown). Data were analyzed with Till Vision and image J softwares.

Viability assay

Cell viability was determined after lipid treatments using CellTiter 96® Aqueous Cell Proliferation Assay (Promega, Madison, WI, USA) according to the manufacturer's instructions. Cells were washed once to remove serum and incubated with lipids for 1 h at 37°C, in DMEM without phenol red. The reagent was added and the absorbance at 490 nm was recorded after 2 hours, using a plate reader (Beckman Coulter, CA, USA). Results were expressed as a percentage of untreated control cells taken as 100%.

Fly stocks

Canton S flies were raised on a standard yeast–glucose–agar medium (Roberts, 1998) and maintained at 23°, 70% relative humidity, in 12-hr light/12-hr dark cycles.

Electrophysiology

Experiments were performed at 20–22° C on Drosophila third body wall dissected in Ca++ free HL3 saline and pinned on the sylgard (Sylgard 184, Dow Corning) coated surface of a 35 mm Petri dish. For electrophysiological experiments, Ca++ free HL3 was replaced with 1 ml Ca++ 0.4 mM HL3 in order

to minimize muscle contractions during segmental nerve stimulation. Single segmental nerves were stimulated (square wave stimuli, 0.15 ms duration x 1.5 threshold voltage) using a suction electrode connected to a Grass S88 stimulator (Grass, USA). Excitatory junctional potentials (EJPs, evoked by nerve stimulation) were recorded intracellularly in muscle fibers 6 and 7 of abdominal segments A2–A4 using glass microelectrodes (0.5 µm tip diameter, 10–15 MΩ resistance) (Science Products, Germany). Only fibers with a resting membrane potential of –60 mV or more were choosen for experiments. Initially, single-pulse stimulations were given at 0.3 Hz frequency in order to reach the threshold voltage. Stimulation frequency was then switched to 10 Hz for the rest of the experiment. After 30 s, SPANs, LysoPC+FA, either LysoPC or FA alone, or an equal amount of control saline were added. Recordings were amplified with a current-voltage clamp amplifier (TEC-05 NPI, Germany), conditioned with a signal conditioner (Cyber Amp, Axon Instruments, USA) and fed to a computer for subsequent analyses via an A/D interface (Digidata 1200, Axon Instruments, USA). Digitized data were analyzed off-line with MiniAnalysis (Synaptosoft, USA) or PClamp 6.04 (Axon Instruments, USA). An average of 3-4 larvae were used.

Immunohistochemistry

Immunohistochemical stainings of third instar larvae body-wall preparations were performed as in [2]. Several immunostainings were performed on 3rd instar larvae, with a polyclonal primary antibody against the presynaptic marker HRP (1:150; Cappel, USA). Primary antibodies were detected with Texas Red-labeled donkey anti-goat antiserum (1:200; S.Cruz, USA,). Bodywall preparations were observed with a Leica ADMIRE3 epifluorescence microscope equipped with a Leica DC500 CCD camera and a 63x oil immersion objective (NA 1.4). Sequential optical sections (0.3 µm thickness) of muscle fibers 6 and 7 NMJs were acquired using Leica FW4000 software (Leica, Germany). Deconvolution of the stacks and reconstitution of the relative maximum projections were performed using Leica Deblur software. Type I bouton areas were measured using ImageJ v1.35 (NIH, USA).

Toxin Labelling and Assay

One hundred fifty micrograms of purified toxin (Ntx, Tpx and Tetx) were resuspended in 150 µl Hepes 10 mM, NaCl 150 mM, pH 7.4; the pH of the reaction buffer was adjusted to 8.0 by adding sodium bicarbonate. Fifteen micrograms of Alexa568 dye (Molecular Probes) (from a stock solution of 10 µg/µl in DMSO) were added to the toxin solution. The reaction was carried out in the dark at room temperature for 1 h under continuous stirring and was stopped by the addition of 15 µl hydroxylamine 1.5 M pH 8.5. Excess dye was removed by extensive dialysis against Hepes 10 mM, NaCl 150 mM, pH 7.4 (Slide-A-Lyzer dialysis cassette, cut off 10 kDa, Pierce). The conjugate was collected, its absorbance spectrum was recorded and ratios of 0.5 Alexa568/Ntx molecule, of 1.2 Alexa568/Tpx molecule and 3.5 Alexa568/Text molecule were determined. The toxicity of Alexa568-conjugated toxins was assayed in the mouse nerve-hemidiaphragm preparation. Alexa568-Tetx showed pronounced absorption onto the poly-lysine/poly-ornythine-laminin coating of the neuronal cultures and could not be used for neuron imaging.

Assessment of Permeability Transition in Isolated Mitochondria

Rat Brain Mitochondria was obtained from adult Wistar rat forebrains as previously described. Onset of the permeability transition was monitored as the fast Ca^{2+} release following accumulation of multiple 10 µM Ca^{2+} pulses at 1-min intervals (Fontaine and Bernardi et al, 1998). Extra-mitochondrial Ca^{2+} concentration was monitored with the Ca^{2+} indicator Calcium Green-5N (excitation/emission, 505/535 nm, Invitrogen) with a PerkinElmer 650-40 fluorescence spectrometer. Mitochondria were resuspended to the final protein concentration of 1 mg/ml in 2 ml of the following medium: 120 mM KCl, 10 µM EGTA, 5 mM glutamate, 2.5 mM malate, 1 mM Tris-phosphate, 10 mM Tris-HCl, pH 7.4, 1 µM Calcium Green-5N. A quartz cuvette with continuous stirring through a magnetic bar was employed to ensure rapid mixing. The number of 10 µM Ca^{2+} pulses retained by the mitochondrial suspension before PTP

opening was counted and set to 100% mitochondrial CRC. Experiments were performed within three hours of mitochondria isolation.

Results and discussion

Effects of different lysophospholipids on the neuromuscular junction

Our previous works underlined the ability of lysoPC, produced by the hydrolysis of PC by SPANs, to paralyse the NMJ. The first question arising from this observation is whether other molecules with similar structure are able to induce analogue modification on neurotransmitter release.

To better understand the lipid effects on neuromuscular junction we tested several lysoPLs with different head polar groups, both zwitterionic (like lysoPE) and negatively charged (like lysoPS, lysoPA, lysoPG, lysoPI)(Caccin *et al.*, 2006). Oleoyl or myristoyl derivatives are used depending on commercial availability.

High Mg (5-7mM)				
	lysoPL		lysoPL+ OA	
	T50%	RP*	T50%	RP*
LPC Myristoyl	10'±3 n=3	100	14'±4 n=7	100
LPC Oleoyl	19'±11 n=5	53 (100)	35'±8 n=5	45 (100)
LPE myristoyl	18'±13 n=3	55	37'±9 n=3	38
LPA oleoyl	79'±48 n=4	8 (24)	188'±13 n=3	7 (19)
LPS oleoyl	172'±49 n=4	6 (11)	177'±52 n=4	8 (20)
LPG myristoyl	230'±99 n=4	4	224'±50 n=4	6

Table 3. Comparison of the NMJ paralysis time induced by different lysoPLs and lysoPls mixtures with OA.The inhibitory activity of lysophospholipids is expressed as the time required to reduce the muscular twitch to 50% of its initial value ($T_{50\%}$). Comparison between the relative potency (RP) of the different lysoPL was made by taking the $T_{50\%}$ of myristoyl-lysoPC as 100%. The same comparison made for the oleoyl derivatives are given in parenthesis.

**RP=relative potency($T_{50\%}$LPC/ $T_{50\%}$ other lipid x 100*

The fatty acid in position 1 influences the effect of the molecule: for lysoPC, the myristoyl derivatives are more potent than their oleoyl counterparts (Rigoni *et al.*, 2005), possibly because of their more pronounced inverted cone shape, due to the shorter hydrocarbon chain, and to their more efficient partition into the plasma membrane. In order to perform a correct comparison we have used both myristoil and oleoyl derivative of lysoPC.

effective.

In physiological buffer (low [Mg^{2+}]), all these lipids are not able to induce paralysis of NMJ, at least when used at concentration and time comparable to that used for lysoPC. Using experimental protocol where muscular twitch is reduced by high [Mg^{2+}], all lysoPLs, added to a final concentration of 150 μM, paralysed the NMJ, although with different potency and kinetic.

The time periods required to achieve 50% muscle paralysis ($T_{50\%}$) are reported in table 3.

The comparison was made between both lysoPLs alone or in equimolar mixture with oleic acid; the presence of OA does not affect (or in some case decreases) the potency of the lysoPL, in contrast with the synergic effect found for lysoPC and OA in physiological buffer. Among the lysoPLs tested here, only lysoPE has a potency comparable to lysoPC, whereas all the others are much less

The major differences related to the kinetic of paralysis. LysoPC and lysoPE paralyse the NMJ with a simple run-down curve and the presence of OA slightly decreases their effect. LysoPA causes a biphasic curve with a rapid initial inhibition which then progresses at a lower rate; its mixture with OA has a very slow effect ($T_{50\%}$ increase more than twice). Finally lysoPS, lysoPI and lysoPG induce a triphasic curve, reminiscent of that elicited by SPANs, but requiring significantly longer time (fig.18).

The first inhibition phase is very similar for all lysoPLs both in time and in amplitude, causing in few minutes a twitch reduction to about 60-70% of its initial value. The second facilitation phase, on the contrary, is very different: lysoPS shows a recovery that range from 110-120% after 30-40 minutes, followed by a slow decrease; preparations treated with lysoPG reaches 130-140% after about 60 minutes and then the twitch clearly decrease up to complete paralysis. Finally, lysoPI is not able to induce neuromuscular paralysis

in our experimental time; it slowly produces a great increment in muscular contraction (up to value of 200%) that in some case starts to decline after 300-400 minutes from the beginning of the experiment.

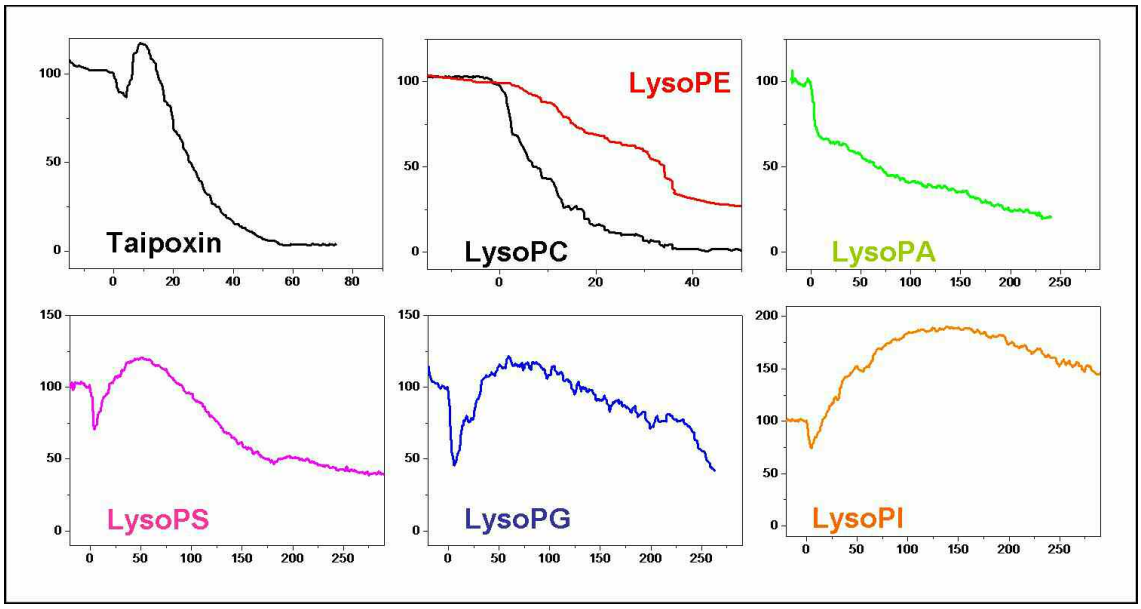

Figure 18. Paralysis of the NMJ caused by different lysoPLs in high [Mg^{2+}] bathing medium. Typical paralysis profiles obtained after addition of the specified lysophospholipid; abbreviations used are as given in the text. The negatively charged lysoPLs cause a rapid depression of the muscle twitch, comparable to phase ① described in fig. 1 for the snake neurotoxins. LysoPS and lysoPG also induced a facilitation phase similar to the phase ② of snake neurotoxins; this later facilitation effect is absent in the case of lysoPA. Zwitterionic lysoPLs (lysoPC and lysoPE) cause a more rapid paralysis of NMJ with a run-down curve. Lipids are added at time 0.

These unexpected results allow to do some consideration related to the mechanism of action of SPANs:

- the initial depression and facilitation of the NMJ function is linked to the presence of high [Mg^{2+}], and therefore is not likely to be present *in vivo*, during envenomation.
- magnesium appears to act on the presynaptic membrane rather than on the SPAN itself, as there are lysoPLs (lysoPS, lysoPG) which mimic the toxin effect, with a triphasic paralysis profile, and high [Mg^{2+}] does not affect the phospholipase A2 activity of SPAN (see page x, our unpublished observations).
- generally, paralysis develops more rapidly in high [Mg^{2+}]
- no lag phase is present in the action of SPAN and of lysoPL in high [Mg^{2+}]

A possible explanation of these data is that Mg^{2+} at high concentrations interacts with the “active zones“ (AZ) of the presynaptic membrane, which are the preferred sites of synaptic vesicle fusion with the plasma membrane, making them more sensitive to membrane fusion with synaptic vesicles.

The implication of AZs in the inhibitory effect of SPANs and lysoPL also offers an explanation for the different lipid behaviour found here with respect to the first inhibitory phase. In fact, lysoPG, lysoPS, lysoPI and lysoPA, possibly owing to their net negative charge, may insert into the AZs and change their structure in such a way as to make them less prone to fuse with synaptic vesicles. On the contrary, the initial lysoPC or lysoPE partition into these zones does not affect their propensity to fuse. When more lysoPC or lysoPE are incorporated into the AZs their effects on membrane curvature develops and then affect exocytosis and endocytosis. The initial inhibitory effect of lysoPG, lysoPS and lysoPA is overcome as more of them are incorporated.

It was proposed that also SPANs bind within the AZs of the presynaptic membrane (Rossetto *et al.*, 2006). Toxin binding to the AZ could accounts for the lack of binding competition among the different SPANs, and, at the same time, for the presynaptic neurospecificity of SPANs. Additionally, it is possible that SPANs display their hydrolytic activity within AZ boundaries where some lipid mismatching and a reduced amount of cholesterol may exist. This suggestion follows the finding that β-bungarotoxin is most active at the liquid crystalline-gel phase transition of phosphatidylcholines and virtually inactive in the presence of cholesterol (Kelly et al., 1979). Different pharmacokinetics and/or different affinities of binding of SPANs to the AZ also account for the poor correlation between their PLA2 activity and toxicity (Montecucco & Rossetto, 2000) and the very large difference in toxicity between SPANs and the pancreatic PLA2. In fact, in this view, binding with consequent strict localization of the PLA2 activity is a major event in the entire intoxication process.

Reversibility of lysoPLs induced paralysis of the neuromuscular junction

The nerve muscle preparation allows to identify also possible muscle alteration induced by treatments tested. Direct muscle stimulation after experiment with lysoPLs elicits a complete muscular response, indicating first of all a presynaptic action of lipids, and then that a permanent damage is not established within the experimental time. If the partition of lysoPL and FA into the presynaptic membrane is responsible for the blockade of the nerve terminals, one would expect that their removal from the membrane would restore synaptic function. Removal of FA and their derivatives can be achieved by addition of albumin, a serum protein which contains several FA binding sites (Simard *et al.*, 2006). Fig. shows a typical twitch profile of the lysoPC+OA-treated NMJ in high [Mg^{2+}]; the simple washing with a lipid-free and albumin containing medium completely restores the nerve-stimulated muscle twitch.

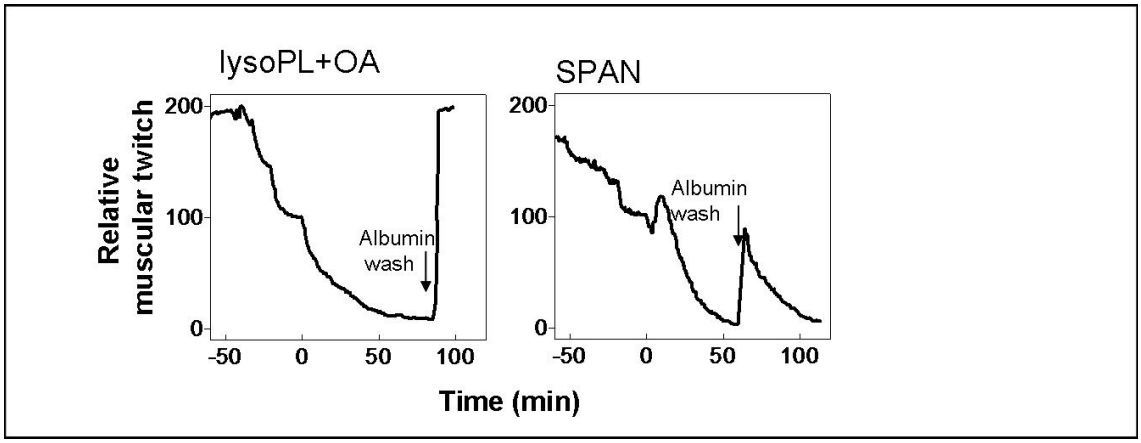

Figure19 . Albumin washing reverses the neuromuscular paralysis induced by SPANs or by lysoPLs. At complete paralysis the bathing medium was replaced with a medium containing 0.2% albumin (arrow) in physiological low [Mg2+] buffer. The albumin washing restored the twitch amplitude to the initial values (left panel). A similar behaviour was obtained after intoxication with all SPANs tested, but in this case the recovery was partial and temporary (right panel).

Recovery of NMJ function is completed within few minutes, suggesting that the lysoPL and FA equilibration between the membrane and the medium and their binding to albumin are very rapid. Similar recoveries were obtained with the

other lysoPL tested here (not shown).

If the NMJ paralysis induced by SPANs is indeed mediated by lysoPL and FA, for the same physico-chemical reasons, albumin washing should be effective also in the case of the SPAN-induced inhibition. Fig. 19 shows that this is indeed the case. However, recovery is only partial and then paralysis progresses again. The same pattern was recorded with all toxins tested in high [Mg^{2+}]. This temporary relief of inhibition is expected on the basis of the known fact that SPAN binding becomes rapidly irreversible, as SPANs cannot be washed away and become insensitive to the action of specific anti-toxin antibodies (Simpson *et al.*, 1993). Thus, the toxin can continue to hydrolyse phospholipids on the presynaptic membrane, with the production of the lysoPL and FA which then again inhibit the synapse.

Comparison of SPANs and their lipid products at the Drosophila melanogaster larval neuromuscular junction

Drosophila melanogaster is a good model to study alteration of neurotransmitter release because of the facility to isolate NMJ and the availability of several mutants defective in exo-endocytosis. We decided to test the four SPANs and their lipidic products, myristoil- LysoPC and oleic acid. Experiments was performed on third instar larval body-wall, in HL3 buffer (Stewart *et al.*, 1994). Segmental nerve stimulation evokes, in larval muscel fibers, a post-synaptic excitatory junctional potential (EJP), without generating any action potential. Under this condition, SPANs do not have any effect on EJPs, even at very high concentration. (fig. 20)

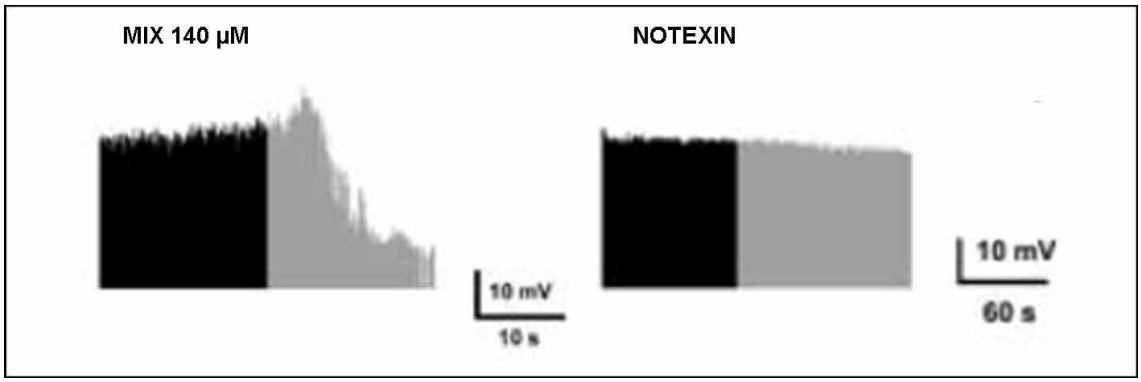

Figure 20: representative traces of evoked EJPs before (black) and after (grey) addition of myristoyl-lysoPC +OA (140 µM) or notexin (50 nM). Resting membrane potential was around -60 mV

On the contary, the mixture myristoyl-lysoPC+OA causes a very rapid inhibition of the neurotransmitter release: at 140 µM the block is complete in 20 seconds; the effect is dose dependent and at lower concentration (60 µM) the profile of inhibition is very similar to that observed in mammalian NMJ: there is an initial increase of neurotransmitter release which is followed by a run-down of the response; the HL3 buffer used for these experiments contains high magnesium concentration (20 mM).

In this model LysoPC is the effective species, and it is able to cause alone the same effect obtained with the mixture; no detectable effect was observed with OA (fig. 21).

Under resting condition, the Drosophila NMJ presents spontaneous neurotransmitter release. A single events of synaptic vesicle fusion produced a miniature excitatory junctional potential (MEJP).

The incubation of the NMJ preparation with the lipid mixture (140 µM) causes a clear increase in the frequency of MEJPs without altering their amplitude, and, also in this case, lysoPC was responsible for this effect.

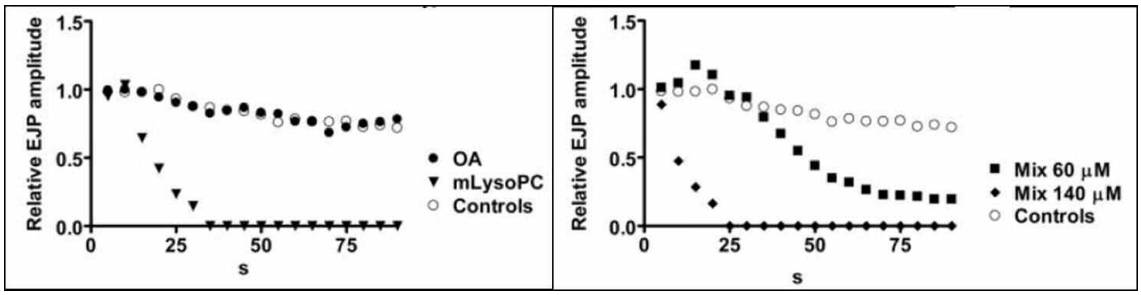

Figure 21: relative EJP amplitude after addition of indicated lipids at time 0. values of each plot represent the mean value ± S.E.M. (covered by symbols) for 5s bins of a sample of three different experiments.

The imbalance between exo and endocytosys, proposed as the mechanism for lipid action at NMJ, is expected to produce also morphological changes, like a swelling of nerve terminal as observed in mammalian NMJ.

Immunoistochemical staining of body-wall preparation was performed before and after treatment with 30 µM lipid mixture and the area of nerve terminal bouton was measured.

The average size after lipids incubation is significantly higher than that of the control, as shown in figure 22.

The results obtained significantly differ from that at the mouse NMJ. Whilst lysoPC is an effective inhibitor of D. melanogaster motoneuron terminal, SPANs are non effective on this model. These results indicate that the nerve terminal binding of such neurotoxins is a prerequisite for their activity (Megighian *et al.*, 2007).

The evolutionary implications of this finding is noteworthy because it underscores the likely evolutionary pressure exerted on snake neurotoxins in order to adapt to the molecular components of the nerve terminals present in their usual vertebrate preys. On the other hand, the block of neurotransmission

induced by lysoPC seems to derive from a general mechanism, shared by vertebrate and invertebrate.

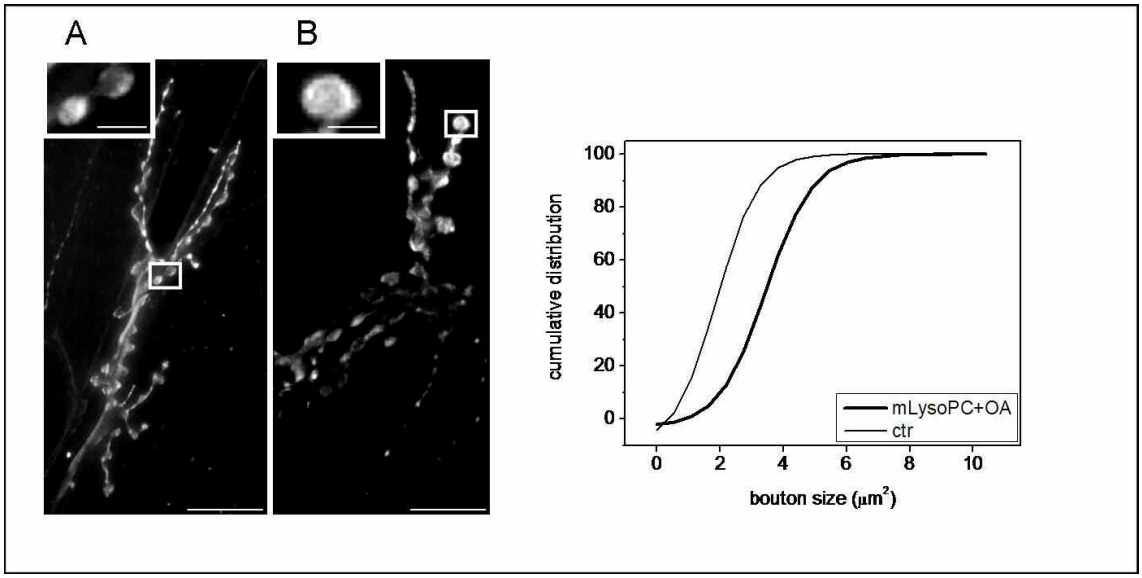

Figure 22: Drosophila larvae neuromuscular junction before (A) and after (B)treatment with myristoyl-lysoPC+OA, 30 µM final concentration, stained with anti-HRP antibody. Scale bar: 10 µm. Insets: type I boutons at higher magnification (scale bar 2 µm). the graph represents cumulative distributions of boutons areas.

.

Role of salivary lipids and PLA2 activity in insect

Studies on some species of hematophagus arthropodes (Golodne *et al.,* 2003) evidenced the presence in their saliva of significant quantity of lysoPC. The proposed role for this lipid is as anti-hemostatic agent, that cooperate with the complex array of proteins produced by salivary glands in this animals. Very recently (Mesquita *et al.*, 2008) it was also demonstrated the immunosuppressant role of salivary lysoPC from Rhodnius Prolixus: this hematophagus is the vector that transmits the parasite Trypanosoma to human skin, and lysoPC seems to contribute to the infection. It cannot be excluded that lysoPC plays other roles in this context; for example, hematophagus insects, like snakes, can be really assisted by a block of the neuromuscular activity of their preys, that in some case include also small vertebrates such as frogs or little fishes.

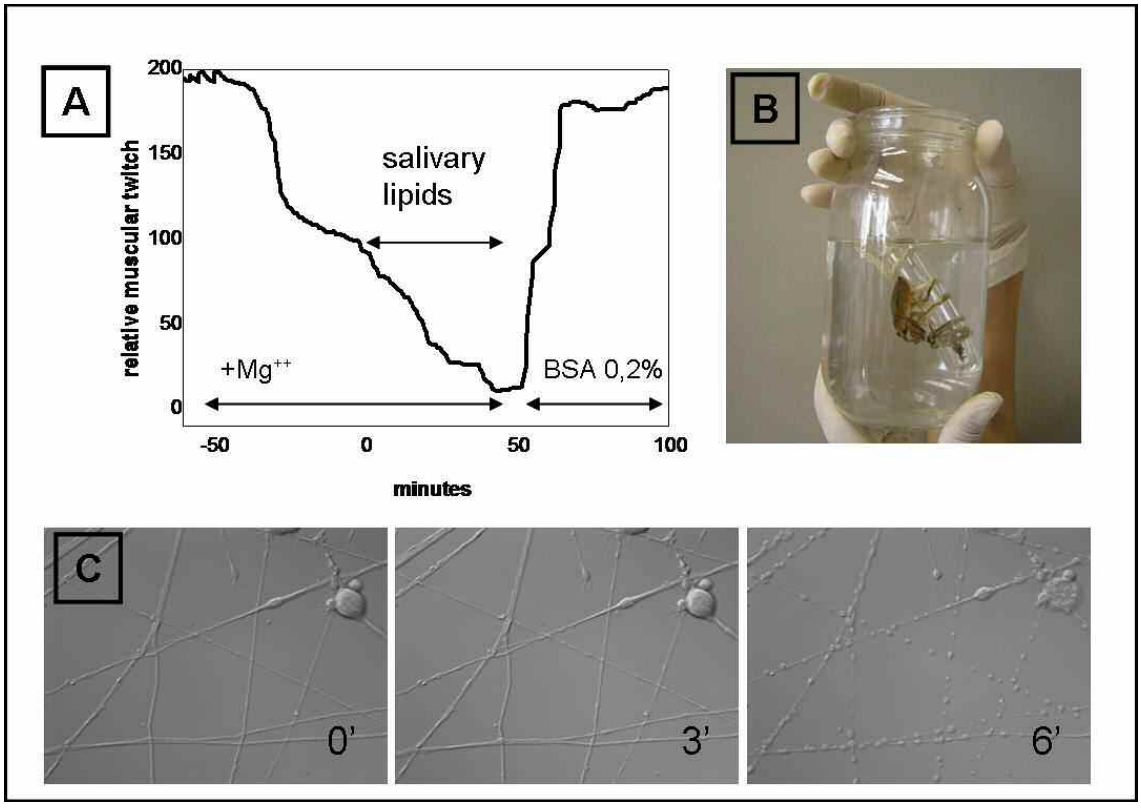

Figure 23: Salivary lipids from Belostoma, added at time 0, induce paralysis on mouse isolated NMJ (A) and bulging of NSC34 cell line (C); the paralysis reverts if muscle was washed with BSA. B: exemplar of Rhodnius Prolixus.

We decided to test in our experimental models if salivary lipids are able to induce similar effects to that obtained with synthetic lipids.

Lipidic extracts from saliva of Rhodnius Prolixus and Belostoma (Giant water bug), obtained by the group of prof. G. Atella (Universidade Federal do Rio de Janeiro, Brazil), were tested in mouse nerve-hemidiaphragm preparations and in neuronal cellular models.

As shown in figure 23, 50 µM salivary lipids rapidly paralysed the mouse NMJ, and the paralysis was fully reversed by albumin wash. On NSC34 cell line and spinal cord motorneuron the formation of bulges along neurites are observed; both experiments had a kinetic very similar to that of synthetic lysoPC at the same concentration.

These results are in good agreement with the hypothesis that lysoPC in insect saliva acts as a very simple form of venom, generated by digestive enzymes. Clearly, the effect is related to the dose injected, but the mechanism of paralysis could be effective on a broad spectrum of little sized preys. Moreover, hematophagus insects have in their saliva enzymes with PLA2 activity (G. Atella, personal communication) that they can use to generate lysoPLs. Snake neurotoxins are evolved from digestive PLA2, and it is possible that they conserve a common mechanism of action (the production of lysoPLs as blocking agents), greatly enhanced by a new, specific capacity of binding and localisation.

Intracellular calcium increase induced by SPANs and lipid mixtures

Cells intoxicated by SPANs or treated with lipid mixtures show an almost completely loss of synaptic vesicles, effect that overcome the simple fusion of the ready-releasable pool (RRP). Such extensive vesicle fusion can be caused by a rise in intracellular calcium concentration ($[Ca^{2+}]_i$).

Two types of neuronal primary cells (CGNs and scMNs) loaded with the ratiometric calcium indicator Fura-2, were used to test if variation in $[Ca^{2+}]_i$ are implicated in the mechanism of neurotoxicity induced by SPANs and by their enzymatic products.

$[Ca^{2+}]_i$ significantly and progressively increases in the bulges after toxins application; in contrast, cellular bodies remain almost unaltered during the observation time, as shown in figure. Similar results were obtained for all SPANs tested (Rigoni *et al.*, 2007).

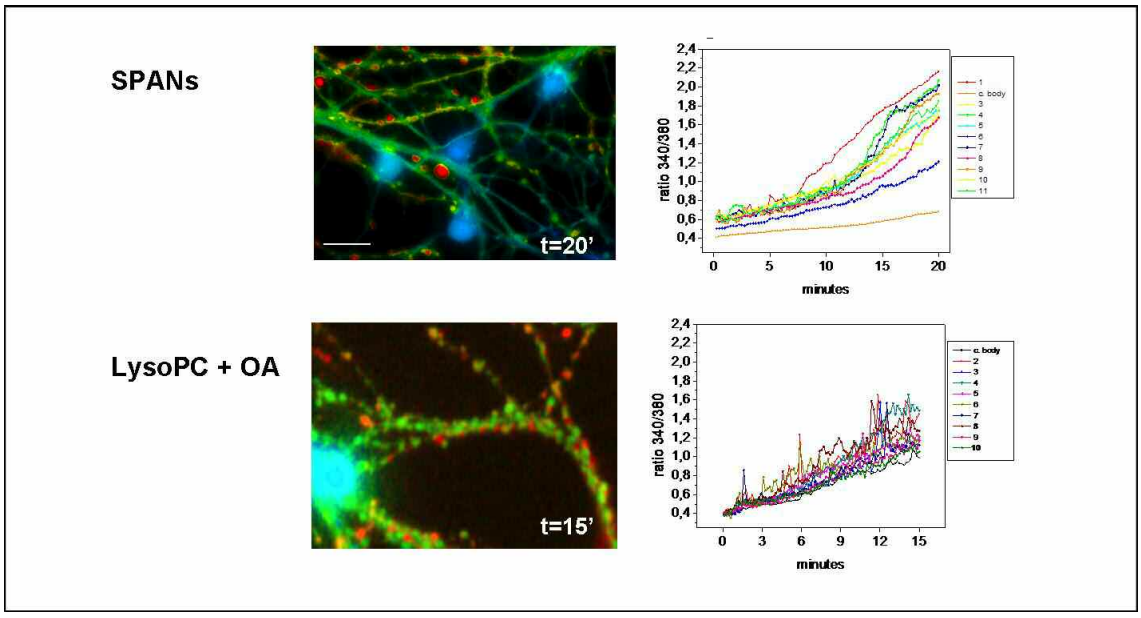

Figure 24: pseudocolor images of CGNs loaded with Fura2-AM and treated with 25 nM taipoxin (upper part) or lysoPC+OA mixture. Calcium concentration increase from blue to red. Scale bar, 10 µm. Graphs report the time courses of changes in 340/380 fluorescence ratios of selected region of interest. These experiments are representative of many performed with different neuronal cultures; for each experiment several different nerve bulges were tracked at the same time.

A comparable increment in $[Ca^{2+}]_i$ was observed also in cells incubated with lipid mixtures (25 µM final concentration). In this case a similar behaviour was detected at the level of cell bodies, and the relative graph was characterized by the presence of repeated spikes. The component of the mixture most effective in raising the $[Ca^{2+}]_i$ is lysoPC; OA, when added alone, has no effect. However, the two molecules clearly synergize in order to produce the effect shown by the mixture in figure 25. This finding parallels the effects that the lipid mixture and the two lipids alone have on the neuromuscular junction of the hemidiaphragm preparation.

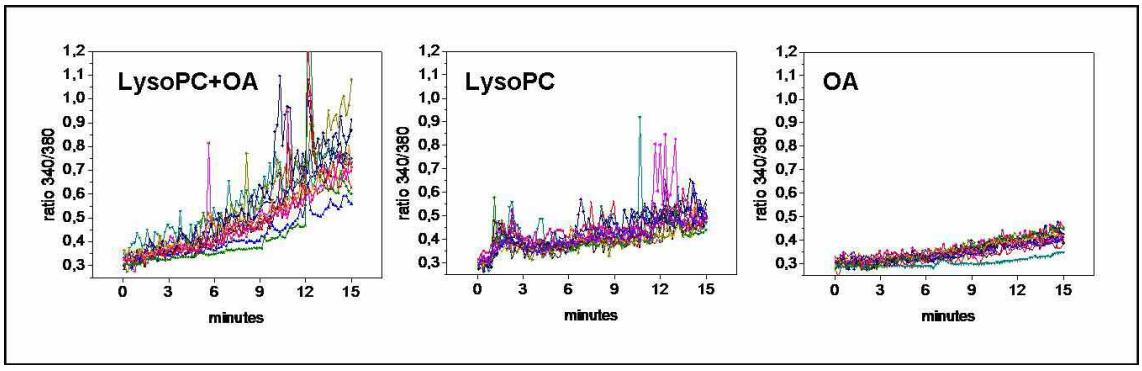

Figure 25: CGNs exposed to indicated lipids, added at time 0 (final concentration 25 µM). Traces showed refer to experiments performed on the same cell culture and are representative of three different sets of experiments

The ability of the lipid mixture to increase $[Ca^{2+}]_i$ both in bulges and cell bodies, compared with the restricted action of SPANs on neurites, could be expected on the basis of the fact that lysoPC and FA can partition into the plasma membrane at any site, whereas SPANs bind specifically to the presynaptic membrane of nerve terminals. On the other hand, the larger $[Ca^{2+}]_i$ increase in the presynaptic regions compared with the cell body could also be influenced by the different surface/volume ratio of the two compartments. Any modification of the homeostatic mechanisms controlling $[Ca^{2+}]_i$ at the plasma membrane is expected to cause substantial variations in the tiny cytosolic rim of the presynaptic membrane, whereas the same modification should take longer to affect the bulk $[Ca^{2+}]_i$ in the cell body.

To analyse the source of calcium increment the experiments with lipid mixtures were repeated in calcium-free buffer. SPANs could not be used in these tests as Ca^{2+} is strictly required for their phospholipase activity. Under this condition the $[Ca^{2+}]_i$ increase was nearly abolished, and only at late time points a very small $[Ca^{2+}]_i$ rise was observed. These data suggest that the main part of calcium increase derive from the extracellular medium, with a minor contribute from intracellular stores.

In order to investigate the nature of Ca^{2+} influx through the plasma membrane, the involvement of voltage-gated Ca channel (VDCC) was tested; neurons were incubated with the P/Q and N-type VDCC inhibitor ω-conotoxin MVIIC (3 µM) and with the L-type inhibitor nimodipine (1 µM). This treatment did not prevent the rise of [Ca2+]i caused by the lipid mixture, although a very small reduction in the rate of [Ca2+]i increase was observed in some neurons treated with these VDCC inhibitors.

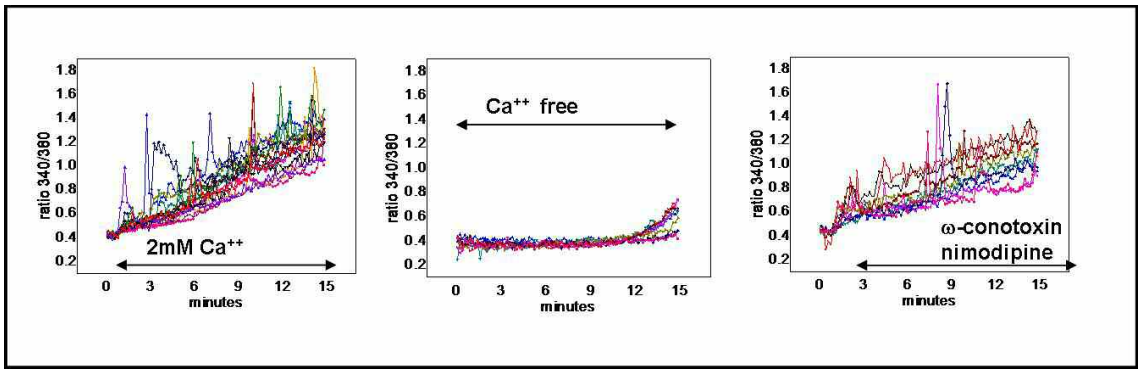

Figure 26: CGNs exposed to 25 µM lysoPC+OA, added at time 0, in physiological buffer (2mM Ca++) or in presence of EGTA (Ca++ free), or with 3 µM ω-conotoxin MVII C and 1µM nimodipine . Traces showed refer to experiments performed on the same cell culture and are representative of three different sets of experiments

Using isolated neuromuscular junction preparations, whose VDCCs are well characterized and known to be effectively inhibited by ω-conotoxin MVIIC, any change in the paralysis time induced by SPANs was observed (see introduction, pg 24).

Control experiments performed with neurons treated with these channel inhibitors and depolarized with 55 mM KCl showed about 50% reduction in the

calcium influx (not shown) Taken together, these results indicate that these synaptic VDCCs may contribute to the rise of [Ca2+]i induced by SPANs in primary cultures of neurons but are clearly dispensable. One possible explanation is that lysoPC-OA induces in cultured neurons a non specific increase in the membrane permeability for small molecules, as it was shown to occur for cultured vascular smooth muscle and endothelial cells (Leung 1998, Woodley 1991) and in lymphoma cells (Wilson-Ashworth 2004). These leaks must be small or specific, since no leakage of Fura-2 (756 Da) was detected during treatment with SPANs or lysoPC-OA.

Another mechanism that can contribute to increase $[Ca^{2+}]_i$ is the impairment of its efflux systems. The efficiency of Ca^{2+} extrusion can be evaluated by chelating extracellular Ca^{2+} after a stimulus that causes increment of $[Ca^{2+}]_i$: the rate of $[Ca^{2+}]_i$ decrease is indicative of Ca^{2+} efflux. In physiological condition this rate is very high, whereas in cells treated with lipid mixtures the efflux is clearly slowed down (fig. 27).

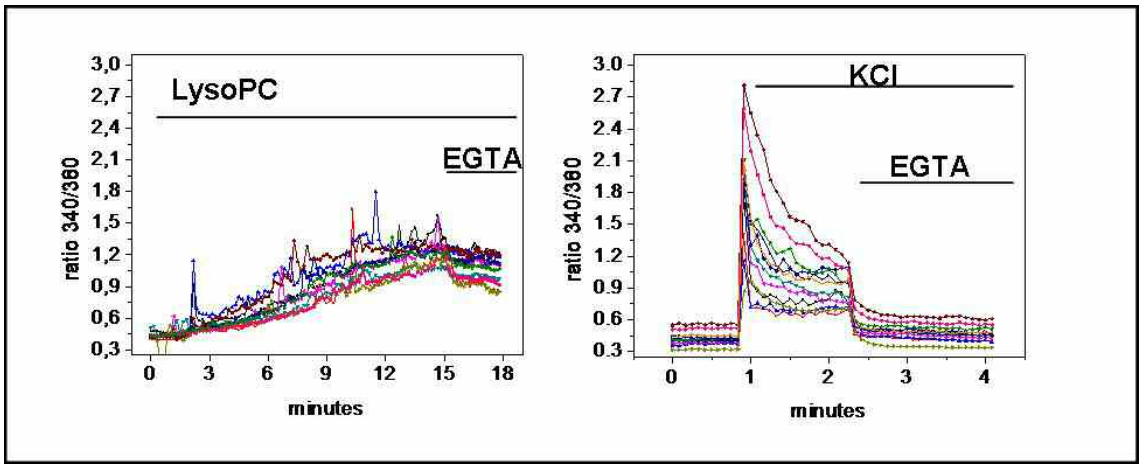

Figure 27: effect of EGTA oncalcium concentration in CGNs treated with 25 µM lysoPC or stimulated with KCl.

Involvement of mitochondria in the mechanism of SPANs action.

Previous studies indicates that SPANs can gain access to the cell interior; indeed, fluorescein-coniugated β-Btx was found to enter in hippocampal neurons in culture (Herkert et al, 2001) and taipoxin was found to localize inside chromaffin cells in culture by antibody labeling (Neco et al, 2003). SPANs required calcium for their hydrolytic activity; the increment in intracellular [Ca^{2+}] that they cause (described in the previous paragraph) suggest the possibility that these enzymes can be active also in the cytosol (Rigoni *et al.*, 2008). Alexa568 fluorescent derivatives of notexin, taipoxin and textilotoxin were prepared; a commercial fluoresceinated β-Btx was used; the toxicity of the fluorescent proteins was tested on isolated NMJ: they were nearly as active as the native toxins.

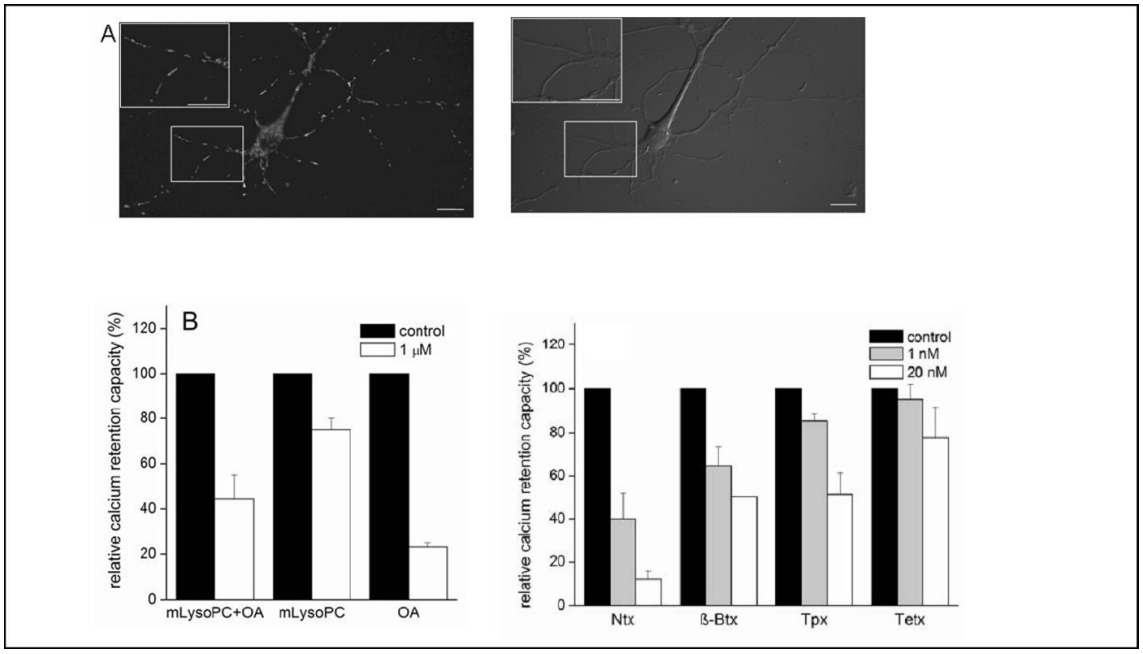

Figure28: A) Intracellular localization of Alexa568-Ntx in spinal cord motorneurons after 5' incubation at 37°C (50 nM). Right panel: the correspondent brightfield. The insets show selected areas at higher magnitude. Scale bar: 10 μm B) Effect of SPANs and PLA2 activity products at different concentrations on Ca^{2+} uptake of purified rat brain mitochondria. Mitochondria were resuspended as described in methods and CRC was tested in the presence of indicated lipids (1 μM) or of the four snake neurotoxins at high (20 nM, white bars) and low (1 nM, gray bars) concentrations. Data represent mean CRC values of intoxicated mitochondria normalized to control samples (black bars). For each condition trials were performed in triplicate

Fluorescent derivatives were used to monitor toxin localization during cellular intoxication. Fig. shows that Alexa568-Ntx rapidly entered neuronal projections of SCMNs. Remarkably, fluorescent neurotoxin was not homogeneously distributed in the cytosol but rather localized to elongated, spaghetti-like structures that are clearly reminiscent of mitochondria (fig. 28A).

A similar staining pattern was found also in cerebellar granular neurons and with Alexa568-Tpx and fluoresceinated-β-Btx (not shown), indicating that the mitochondrial-like staining is a rather general feature of SPANs. Moreover, a clear colocalisation was found between conjugated toxins and nonyl acridine orange, a specific mitochondrial dye. Fluorescent textilotoxin was strongly absorbed by the culture plate coating and could not be used for fluorescence imaging. The effect of SPANs on isolated rat brain mitochondria was then tested. A common cause of mitochondrial swelling and depolarization in situ is the opening of the mitochondrial permeability transition pore (PTP), an inner membrane high-conductance channel that can be desensitized by cyclosporin A (CsA) (Bernardi *et al.*, 2006). The propensity of the PTP to open in a population of mitochondria can be monitored with a sensitive technique based on the calcium ritention capacity (CRC), i.e. the amount of Ca^{++} that can be taken up by mitochondria in the presence of inorganic phosphate before onset of PTP opening. Untreated, control mitochondria accumulated 10 pulses of 10 μM Ca^{++} before onset of the permeability transition, which is readily detected by a precipitous release of the previously accumulated Ca^{++} .

The effects of the four SPANs on the CRC, and their relative potency was tested (fig 28B). Ntx was the most effective, β-Btx and Tpx displayed an intermediate PTP sensitizing activity whereas Tetx was nearly ineffective; this order of potency well correlates with the PLA2 activity of toxins. Moreover, the mixture lysoPC+OA facilitated PTP opening, and OA was in this case the more active component. The action of SPANs on the mitochondrial PTP channel well accounts for the rounding and swelling of mitochondria detected by electron microscopy in intoxicated neurons.

.

Paralysis of the neuromuscular junction induced by miltefosine, perifosine and lysoPAF

The first approach used to evaluate the effects of inverted-cone shaped lipids on neurotransmission consists in measuring their $T_{50\%}$ in mouse nerve-hemidiaphragm preparations. An initial screening was conduced with both lipids alone or in equimolar mixtures with OA, at the same concentration previously used for lysoPC (150 µM). These experiments showed that all the three lipids tested are able to paralyse the NMJ (Caccin *et al.*, 2008); the presence of OA did not modify the profile of paralysis and slightly decrease the $T_{50\%}$, so further experiments were carried on only with the single lipids alone .

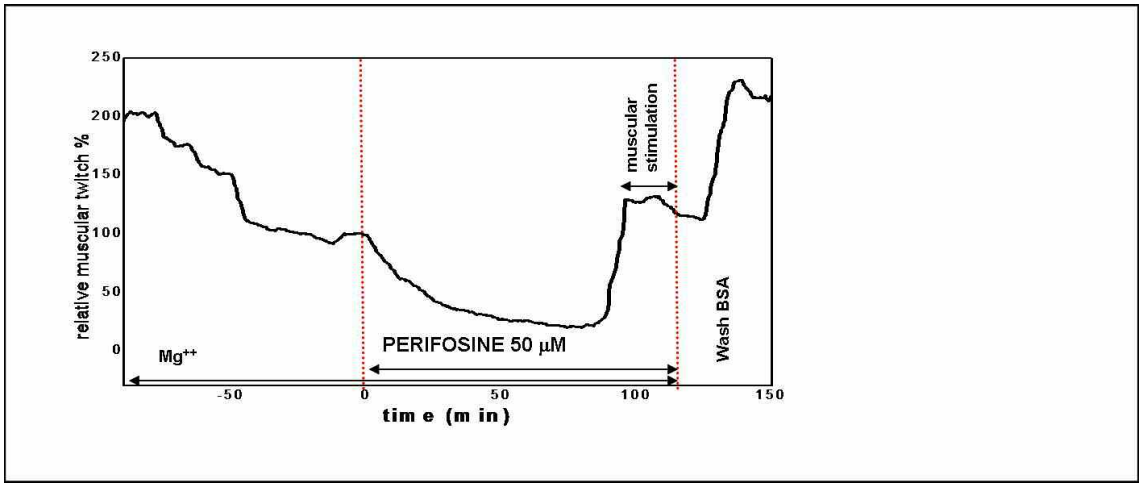

Figure 29: representative profile of paralysis induced by perifosine 50 µM, added at time=0, showing the reduction of muscular twitch by Mg^{++}; the progressive decrement of muscular twitch after addition of perifosine; the direct stimulation of the muscle in presence of perifosine to assess muscular functionality; the restored muscular twitch (nerve stimulation) after wash the preparation with BSA 0,2% . Similar traces were obtained with the other three drugs.

Figure 29 shows the progressive paralysis induced by perifosine, which does not cause by itself any impairment to muscle contraction, as direct electrical stimulation of the muscle elicited full contraction in its presence. The drug must have therefore acted at the level of the nerve terminals. The paralysis is fully reversed by the addition of 0.2% BSA, which binds the amphipatic substances

and restores the normal situation. The same results were obtained with miltefosine and lysoPAF and well reproduces the data already obtained with lysoPC. The neuroparalytic activity of the four different compounds, compared in term of the $T_{50\%}$ parameter, was determined as a function of the concentration, showing that perifosine, miltefosine, lysoPAF and lysoPC have similar neuroparalytic potencies (fig. 30). The impairment of neurotransmission is complete also at the lower concentration (2 µM), but a mild difference can be noticed here: miltefosine and lysoPAF had a faster action with respect to lysoPC,, while perifosine $T_{50\%}$ was shorter but not significantly different.

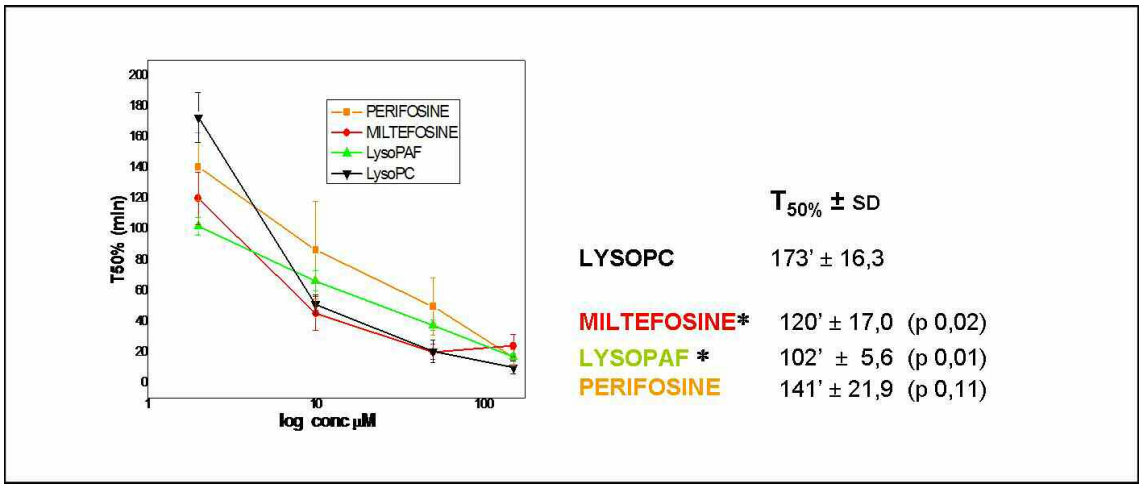

Figure 30: dose/response of the paralysis induced by the four drugs. The ability to induce paralysis is expressed as T50%. Data are the mean of at least 3 experiments and bars represent standard deviation. Statistical analysis was performed by two sample independent t-Test at the 0,05 level of significancy.

These data are consistent with the possibility that the neuroparalytic activity of inverted-cone shaped lipids is mainly due to their insertion into the lipid bilayer of the presynaptic membrane which becomes more fusogenic.

Morphological alteration produced on cellular models by inverted-cone shaped lipids.

SPANs and their lipidic products caused an extensive bulging of neurites in various type of cultured neurons, such as cerebellar granule cells (CGNs) (Rigoni *et al.*, 2004), ippocampal neurons (Bonanomi *et al.*, 2005) and spinal cord motorneurons (SCMNs) (Rigoni *et al.*, 2007). The effect of miltefosine, perifosine, lysoPAF and lysoPC was evaluated on rat SCMNs and on an immortalised cell line, NSC34, hybrid from motorneurons and a neuroblastoma (Cashman *et al.*, 1992).

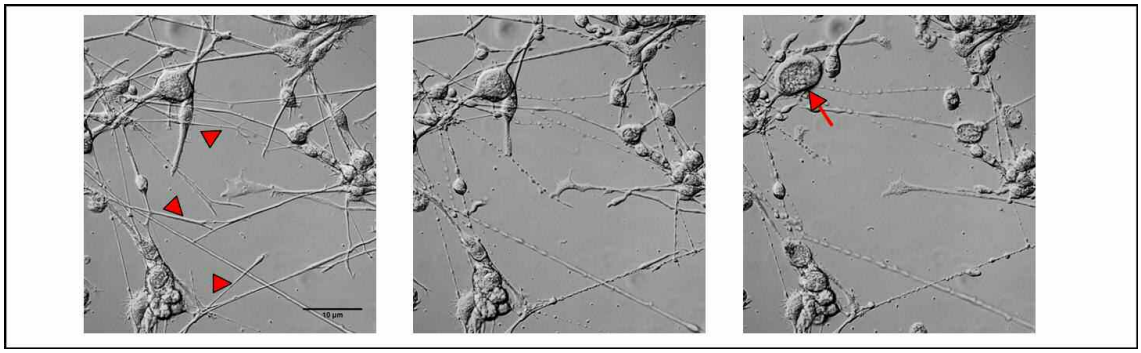

Figure 31: time course of NSC34 cells treated with miltefosine 20 µm. Some neurites(red arrowheads) completely detach from the plate coating. After few minutes cell bodies are greatly damaged (arrow).

The phenomenon of bulges formation is accompanied by a progressive detachment of neurites and cell bodies from the matrix (see fig), that is strictly dependent on the lipidic concentration added to the cells, and in some case can hide it; cellular bodies can be also damaged. This problem has been already observed in previous experiments with lysoPC, but it is more evident with this group of lipids. The concentration range that allows one to observe the bulges formation avoiding damage of neurons is small; so, for each set of experiments, it is necessary to follow this process at the minimum concentration needed to produce a clear effect on cells. All the molecules tested induced bulging along almost all neurites, both in NSC34 and in primary neurons. The swelling develops in discrete points of neurites, and starts almost contemporary in all cells; then the process proceeds increasing the size of bulges, whereas their

number remain constant. For miltefosine, perifosine and lysoPAF a final concentration of about 10 µM induce bulging in 3-6 minutes (fig.32), whereas 15 µM of lysoPC is needed to have almost the same effect .

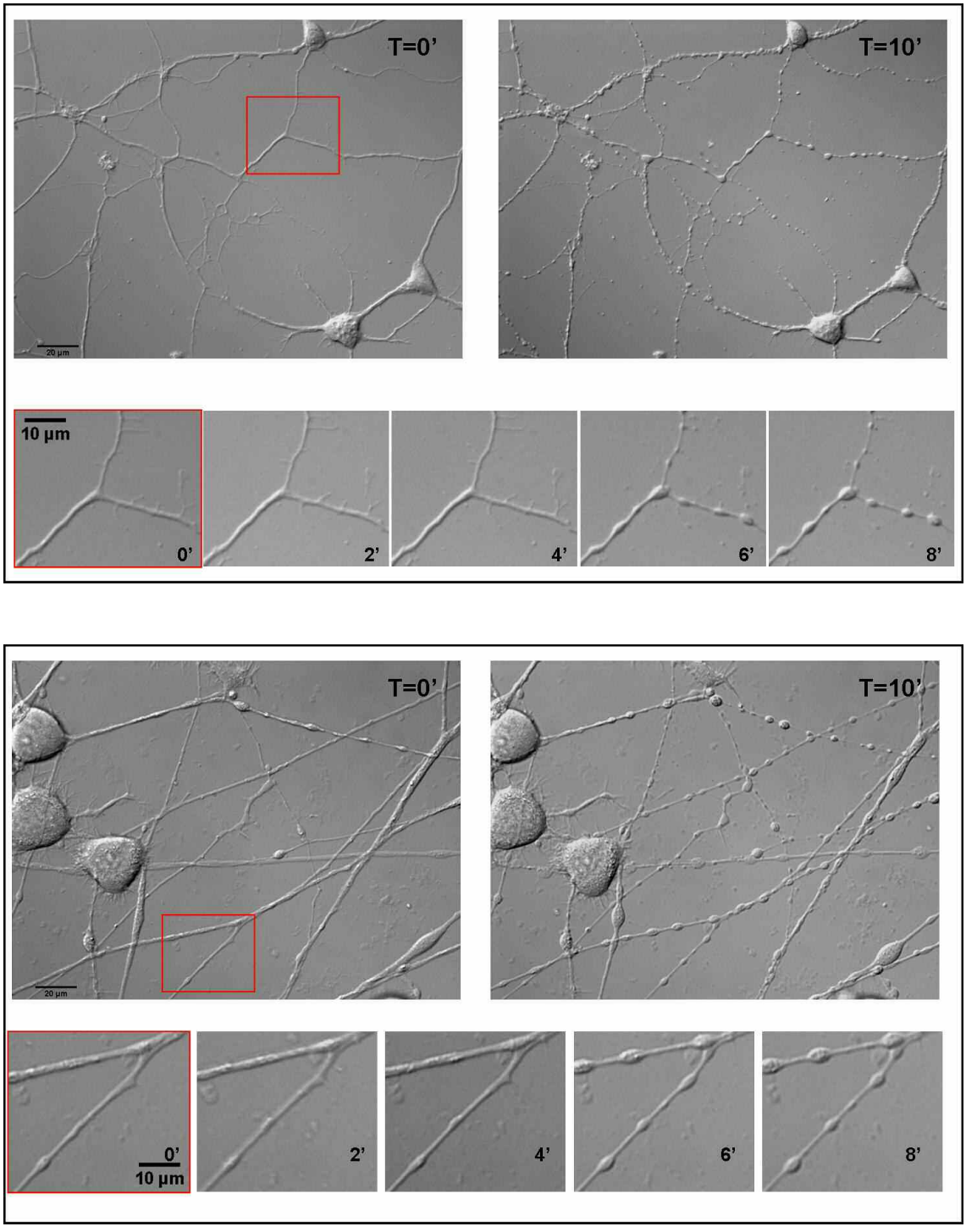

Figure 32: morphological alterationss of spinal cord motorneuron (A)or NSC34 cells treated with alkil lipids. Scale bars10 µm.

Bulging is a neuronal pathological phenotype which can be reversed in cultured neurons by treatment with BSA, similarly to what occurs at the neuromuscular junction. This is the case also here (fig.33). This result supports the conclusion that the insertion into the plasma membrane of inverted cone-shaped molecules, whichever their nature is, causes an alteration of the membrane curvature favouring the fusion of SV.

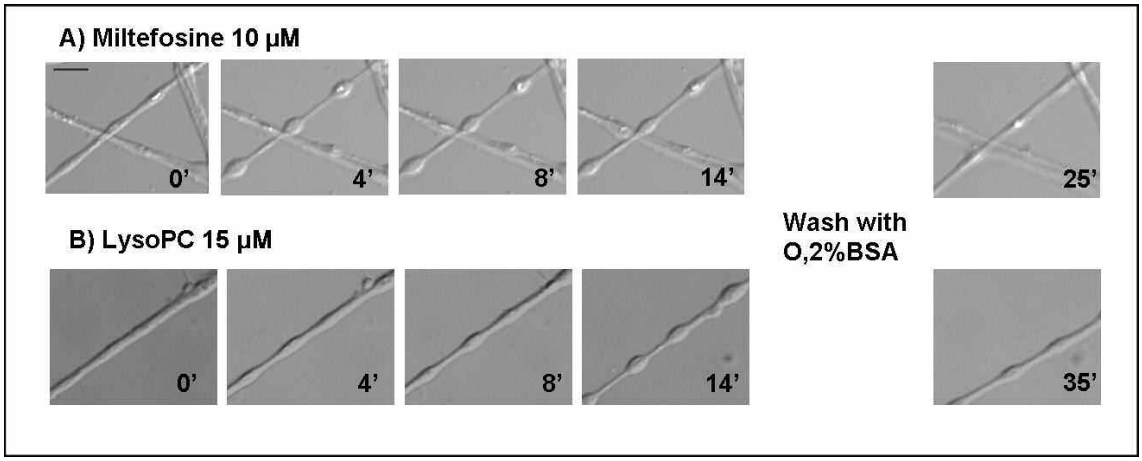

Figure 33: reversibility of bulging induced by alkil lipid after wash with o,2 % bovine serum albumin. Scale bar 10 µm.

Effect of miltefosine, perifosine and lysoPAF on intracellular calcium levels and cellular vitality

Previous work has demonstrated the role of calcium in the alterations typical of SPANs and LysoPC treated neurons (Rigoni *et al.*, 2007). If this is mainly due to the insertion of inverted-cone shaped molecules in the plasma membrane, a similar effect is expected for the other drugs studied.

Using the ratiometric calcium indicator Fura-2 the intracellular calcium concentration ($[Ca^{2+}]_i$) was monitored after the addition of miltefosine, perifosine, lysoPAF and lysoPC. As shown in figure 34 all lipids (5 µM) induces the $[Ca^{2+}]_i$ increase in a spiking mode.

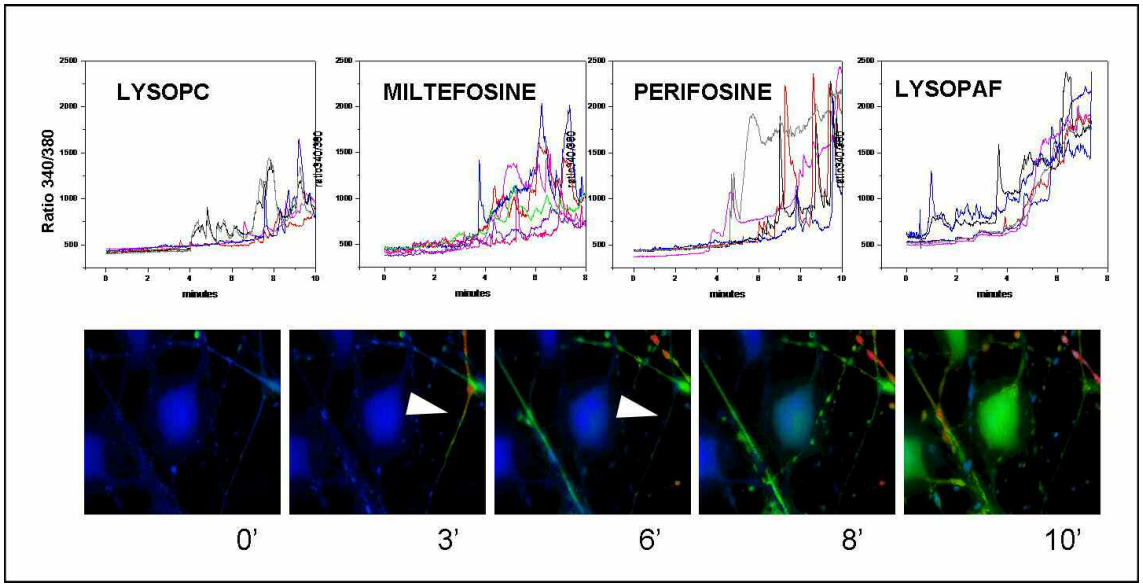

Figure 34. Upper part :representative graphs of calcium increment in NSC34 cells after addition of alkil lipids. Calcium levels are expressed as340/380 fluorescence ratio of Fura2. Lower part: pseudocolors representations of cells loaded with Fura2; arrowheads indicate a neurite where the spiking is clearly shown .

Spikes appear after a lag phase of 3-5 min, similar to that observed for the formation of bulges; they are irregular both in size and timing, as if they were the result of a transient increase of the membrane permeability to external calcium. Some other experiments were performed to better understand the mechanism of calcium increment and figure 35 reports representative results obtained with miltefosine. The addition of EGTA abolishes cytosolic $[Ca^{2+}]$

spiking (panel B), whilst it does not affect intracellular calcium stores which discharge normally upon addition of ionomycin (panel C).

It is possible that the four drugs activate calcium channels of the plasma membrane in such a way as to cause multiple and subsequent opening events. A general inhibitor of plasma membrane calcium channels is millimolar Ni^{2+} (Hille, 2001; Tottene et al., 2000). Indeed, the presence of 4 mM Ni^{2+} in the culture medium completely prevented the opening of the voltage-gated calcium channels induced by membrane depolarization with external KCl (panel E). However, Ni^{2+} did not have any effect on the cytosolic [Ca^{2+}] entry induced by miltefosine (panel F). A similar behaviour was obtained for all the four lipids.

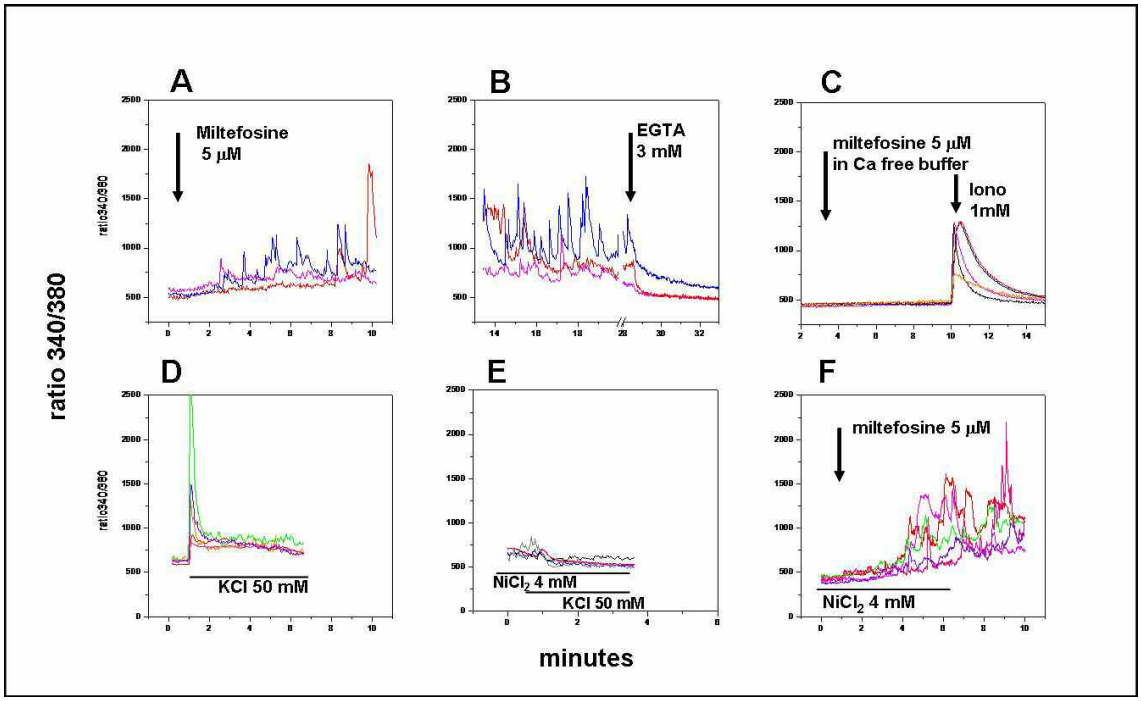

Figure 35: analysis of source and mechanism o calcium increase produced by alkil lipids. See text for details.

As already described for morphological analysis, lipids concentration is a critical parameter since also small increments can greatly damage neurons, depending probably on the detergent effect that this anphipatic molecules can exert. Single cell analysis, like calcium imaging with Fura-2 fluorescence, could be compromised if the cellular population is not completely healthy.

Cellular vitality in the presence of increasing concentration of lipids was determined with a colorimetric method both on NSC34 cells, used for calcium imaging experiments, and in other two neuronal cell lines (Neuro2A and SHSY5Y).

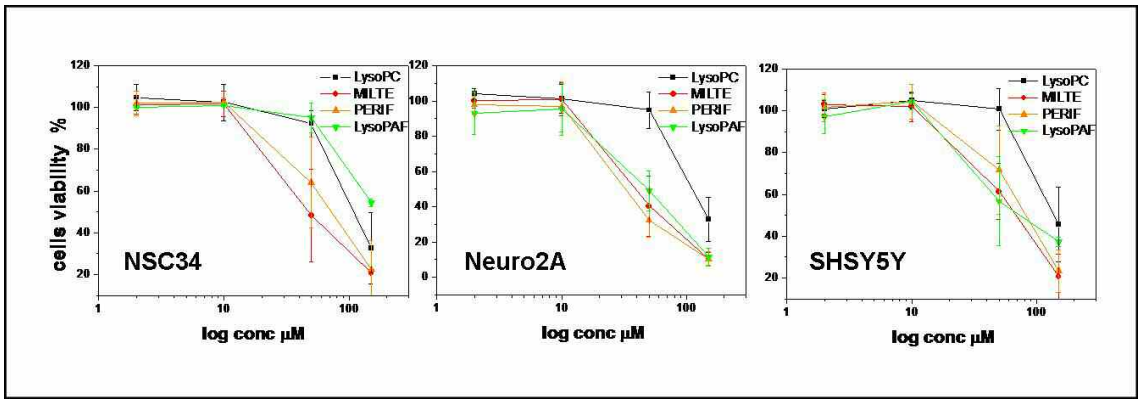

Figure 36: dose-response of cytotoxic effect of lipids. Untreated cells are taken as 100% of live cells. Data reported are the mean of at least three independent experiments ± standard deviation.

No sign of decreased cell viability was detected after an hour from the addition of any of the four drugs tested here, at concentrations (up to 10µM) exceeding those used in the calcium imaging experiments. Closely similar results were obtained also with epithelial cells (Hela, not shown). Only at the high concentrations (50 and 150 µM) a decreased viability was recorded, with miltefosine being the most toxic and lysoPC the least toxic. This finding is in good agreement with the results obtained in other experiments: the behaviour of alkyl lipids is qualitatively closely similar to that of lysoPC but only slightly more potent.

The spiking of cytosolic calcium can be interpreted as the transient opening of lipidic pore on the plasma membrane. These pores are transient because they are formed by membrane lipids and drug molecules which are highly mobile in the membrane plane (fig 37B). These lipid pores allow a rapid increase of the cytosolic [Ca^{2+}] and then close allowing the cytosolic [Ca^{2+}] controlling mechanisms to enter in action thus lowering again the cytosolic ion concentration. As these transient pores continue to open, the net result is an

increase of the cytosolic [Ca^{2+}]. However, the cells used here appear to cope with such increase of the cytosolic [Ca^{2+}] because they do not manifest a decreased viability following calcium entry.

All the data obtained (the neuroparalytic activity, the bulging of neurons, the cytosolic calcium increase) suggest that any amphipatic molecule shaped as an inverted-cone is capable of altering the properties of the membrane of a variety of cells with a particular effect on nerve cells, which are extremely sensitive to changes of membrane permeability.

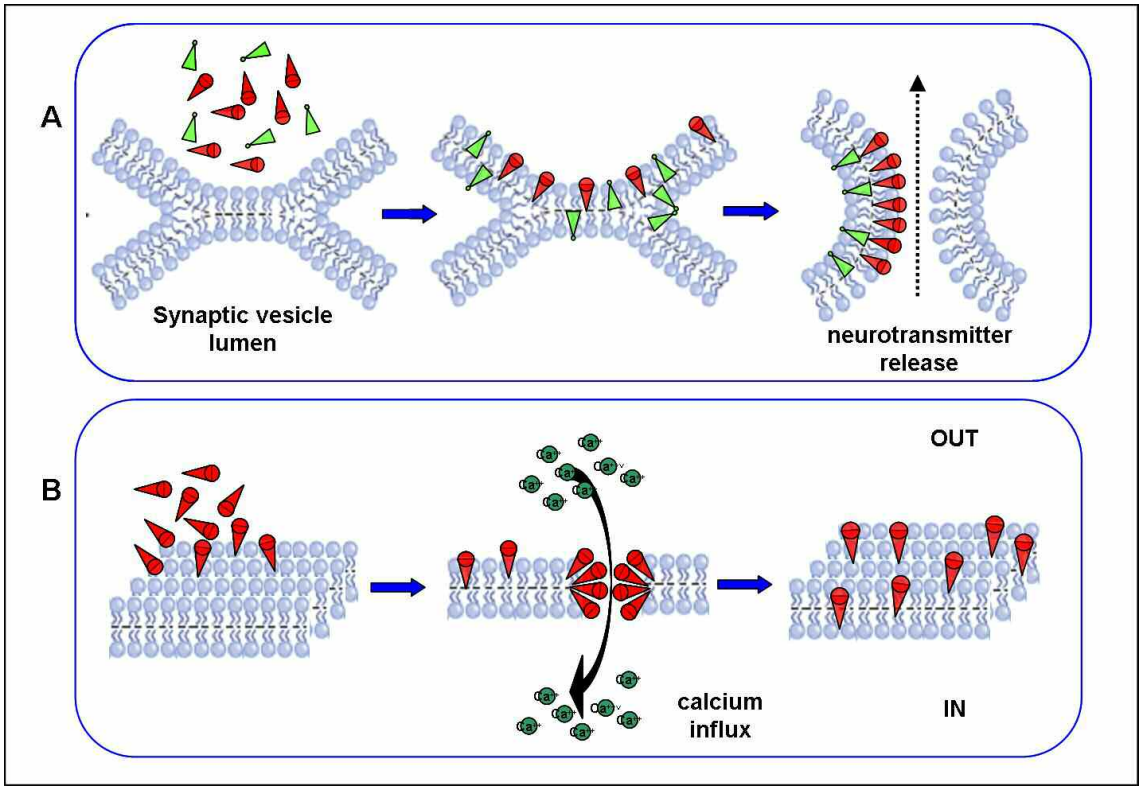

Figure 37: schematic models that summarize the possible effects of inverted cone lipids on presynaptic neurons.

The more evident effect is at the synaptic terminal, where the SV fusion is a very strictly regulated process. Inverted-cone shaped molecules, inserted in the outer layer of the plasma membrane, could greatly affect the release of neurotransmitter and the recycling of synaptic vesicles, by changing membrane curvature and the release probability of SV (fig.37A); moreover, an indirect effect is the increase of the membrane permeability to calcium (fig.37B).

Conclusions

The data presented here contribute to clarify the mechanism of action of SPANs and to highlight the role of membrane lipid composition in synaptic neurotransmission.

The biochemical effectors of SPANs are their hydrolysis products, mainly lysoPC and fatty acids, but their great neurotoxicity is strictly correlate to a specific localization of their enzymatic activity.

The intoxication process can be divided in two phases. In an early stage, toxins bind to (or nearly) active zones, and act on the outer leaflet of presynaptic plasma membrane, exploiting their hydrolytic activity. The main responsible of the first effects observed is lysoPC; various inverted-cone shaped lipids are indeed able, alone, to produce similar effects, promoting the fusion and inhibiting the fission of synaptic vesicles.

In a late stage, toxins seems to enter inside neuron, and to bind to mitochondria; in this phase both hydrolysis products have a crucial role: lysoPLs alter the membrane permeability to calcium, which intracellular concentration arises, promoting further SVs fusion; lysoPLs and oleic acid promote the opening of the mitochondrial permeability transition pore, finally leading to cell death.

Inverted-cone shaped lipids emerge as a class of molecules very effective in the block of neurotransmission, but also, in a more general contest, in the modification of the fusion probability of biological membrane; their action is independent from that of proteins that are involved in this process. This property characterized them as a useful research tool; moreover it suggests also the possibility of their local therapeutic use, for example in superficial hypercholinergic disorders.

Further investigations could be oriented in various directions: an important point is the identification of the molecular receptors of these toxins, known only for β-bungarotoxin; the sequence of events involved in the intoxication need to be still clarify, defining when and where toxins exert their enzymatic action on neurons, and what happens of their products. The use of synthetic fluorescent lipid represents a new approach to asses this question.

Finally, a very interesting field of study derives from the effect of SPANs in vivo: these toxins induce a very rapid, but reversible, nerve degeneration. The mechanisms of the nerve regeneration and the involvement in this process of various cellular component of neuromuscular junction, like Schwann cells, will be analyzed. All these points still underlined the wide possibility linked to the study of neurotoxins.

References

Arce V, Garces A, de Bovis B, Filippi P, Henderson C, Pettmann B, deLapeyrière O.Cardiotrophin-1 requires lifrbeta to promote survival of mouse motoneurons purified by a novel technique. J Neurosci Res 1999; 55:119-126.

Awan KA, Dolly JO.K+ channel sub-types in rat brain: characteristic locations revealed using beta-bungarotoxin, alpha- and delta-dendrotoxins. Neuroscience 1991; 40:29-39.

Bernardi P, Krauskopf A, Basso E, Petronilli V, Blachly-Dyson E, Di Lisa F, Forte MA.The mitochondrial permeability transition from in vitro artifact to disease target. FEBS J 2006; 273:2077-2099.

Bohnert S, Schiavo G.Tetanus toxin is transported in a novel neuronal compartment characterized by a specialized ph regulation. J Biol Chem 2005; 280:42336-42344.

Bonanomi D, Pennuto M, Rigoni M, Rossetto O, Montecucco C, Valtorta F.Taipoxin induces synaptic vesicle exocytosis and disrupts the interaction of synaptophysin i with vamp2. Mol Pharmacol 2005; 67:1901-1908.

Bulbring E..Observation on the isolated phrenic-nerve diaphragm preparation of the rat. British Journal of Pharmacology 1946; 1:38-61.

Caccin P, Rigoni M, Bisceglie A, Rossetto O, Montecucco C. Reversible skeletal neuromuscular paralysis induced by different lysophospholipids. FEBS Lett 2006; 580:6317-6321.

Caccin P, Rossetto O, Montecucco C. Neurotoxicity of inverted-cone shaped lipids. Neurotoxicology 2008; :.

Cashman NR, Durham HD, Blusztajn JK, Oda K, Tabira T, Shaw IT, Dahrouge S, Antel JP.Neuroblastoma x spinal cord (nsc) hybrid cell lines resemble developing motor neurons. Dev Dyn 1992; 194:209-221.

Chernomordik LV, Kozlov MM.Protein-lipid interplay in fusion and fission of biological membranes. Annu Rev Biochem 2003; 72:175-207.

Chernomordik LV, Kozlov MM.Mechanics of membrane fusion. Nat Struct Mol Biol 2008; 15:675-683.

Chioato L, Aragão EA, Lopes Ferreira T, Medeiros AID, Faccioli LH, Ward RJ.Mapping of the structural determinants of artificial and biological membrane damaging activities of a lys49 phospholipase a2 by scanning alanine mutagenesis. Biochim Biophys Acta 2007; 1768:1247-1257.

Cull-Candy SG, Fohlman J, Gustavsson D, Lüllmann-Rauch R, Thesleff S.The effects of taipoxin and notexin on the function and fine structure of the murine neuromuscular junction. Neuroscience 1976; 1:175-180.

Dai H, Shen N, Araç D, Rizo J.A quaternary snare-synaptotagmin-ca2+-phospholipid complex in neurotransmitter release. J Mol Biol 2007; 367:848-863.

Floryk D, Thompson TC.Perifosine induces differentiation and cell death in prostate cancer cells. Cancer Lett 2008; 266:216-226.

Giacomello M, Barbiero L, Zatti G, Squitti R, Binetti G, Pozzan T, Fasolato C, Ghidoni R, Pizzo P.Reduction of ca2+ stores and capacitative ca2+ entry is associated with the familial alzheimer's disease presenilin-2 t122r mutation and anticipates the onset of dementia. Neurobiol Dis 2005; 18:638-648.

Golodne DM, Monteiro RQ, Graca-Souza AV, Silva-Neto MAC, Atella GC.Lysophosphatidylcholine acts as an anti-hemostatic molecule in the saliva of the blood-sucking bug rhodnius prolixus. J Biol Chem 2003; 278:27766-

27771.

Hille B.Ion channels of excitable membranes, Third Edition.Sunderland, Massachusetts :Sinauer Associates, Inc. ; 2001.

Kelly RB, von Wedel RJ, Strong PN.Phospholipase-dependent and phospholipase-independent inhibition of transmitter relase by beta-bungarotoxin. Adv Cytopharmacol 1979; 3:77-85.

Kwong PD, McDonald NQ, Sigler PB, Hendrickson WA.Structure of beta 2-bungarotoxin: potassium channel binding by kunitz modules and targeted phospholipase action. Structure 1995; 3:1109-1119.

Megighian A, Rigoni M, Caccin P, Zordan MA, Montecucco C.A lysolecithin/fatty acid mixture promotes and then blocks neurotransmitter release at the drosophila melanogaster larval neuromuscular junction. Neurosci Lett 2007; 416:6-11.

Mesquita RD, Carneiro AB, Bafica A, Gazos-Lopes F, Takiya CM, Souto-Padron T, Vieira DP, Ferreira-Pereira A, Almeida IC, Figueiredo RT, Porto BN, Bozza MT, Graça-Souza AV, Lopes AHCS, Atella GC, Silva-Neto MAC.Trypanosoma cruzi infection is enhanced by vector saliva through immunosuppressant mechanisms mediated by lysophosphatidylcholine. Infect Immun 2008; 76:5543-5552.

Montecucco C, Rossetto O.How do presynaptic pla2 neurotoxins block nerve terminals? Trends Biochem Sci 2000; 25:266-270.

Montecucco C, Rossetto O.On the quaternary structure of taipoxin and textilotoxin: the advantage of being multiple. Toxicon 2008; 51:1560-1562.

Petan T, Krizaj I, Pungercar J.Restoration of enzymatic activity in a ser-49 phospholipase a2 homologue decreases its ca(2+)-independent membrane-damaging activity and increases its toxicity. Biochemistry 2007; 46:12795-

12809.

Prescott SM, Zimmerman GA, Stafforini DM, McIntyre TM.Platelet-activating factor and related lipid mediators. Annu Rev Biochem 2000; 69:419-445.

Rigoni M, Caccin P, Gschmeissner S, Koster G, Postle AD, Rossetto O, Schiavo G, Montecucco C.Equivalent effects of snake pla2 neurotoxins and lysophospholipid-fatty acid mixtures. Science 2005; 310:1678-1680.

Rigoni M, Paoli M, Milanesi E, Caccin P, Rasola A, Bernardi P, Montecucco C.Snake phospholipase a2 neurotoxins enter neurons, bind specifically to mitochondria, and open their transition pores. J Biol Chem 2008; 283:34013-34020.

Rigoni M, Pizzo P, Schiavo G, Weston AE, Zatti G, Caccin P, Rossetto O, Pozzan T, Montecucco C.Calcium influx and mitochondrial alterations at synapses exposed to snake neurotoxins or their phospholipid hydrolysis products. J Biol Chem 2007; 282:11238-11245.

Rigoni M, Schiavo G, Weston AE, Caccin P, Allegrini F, Pennuto M, Valtorta F, Montecucco C, Rossetto O.Snake presynaptic neurotoxins with phospholipase a2 activity induce punctate swellings of neurites and exocytosis of synaptic vesicles. J Cell Sci 2004; 117:3561-3570.

Rossetto O, Montecucco C.Presynaptic neurotoxins with enzymatic activities. Handb Exp Pharmacol 2008; :129-170.

Rossetto O, Morbiato L, Caccin P, Rigoni M, Montecucco C.Presynaptic enzymatic neurotoxins. J Neurochem 2006; 97:1534-1545.

Schiavo G, Matteoli M, Montecucco C.Neurotoxins affecting neuroexocytosis. Physiol Rev 2000; 80:717-766.

Simard JR, Zunszain PA, Hamilton JA, Curry S.Location of high and low affinity

fatty acid binding sites on human serum albumin revealed by nmr drug-competition analysis. J Mol Biol 2006; 361:336-351.

Simpson LL, Lautenslager GT, Kaiser II, Middlebrook JL.Identification of the site at which phospholipase a2 neurotoxins localize to produce their neuromuscular blocking effects. Toxicon 1993; 31:13-26.

Stewart BA, Atwood HL, Renger JJ, Wang J, Wu CF.Improved stability of drosophila larval neuromuscular preparations in haemolymph-like physiological solutions. J Comp Physiol [A] 1994; 175:179-191.

Tottene A, Volsen S, Pietrobon D.Alpha(1e) subunits form the pore of three cerebellar r-type calcium channels with different pharmacological and permeation properties. J Neurosci 2000; 20:171-178.

Vink SR, van Blitterswijk WJ, Schellens JHM, Verheij M.Rationale and clinical application of alkylphospholipid analogues in combination with radiotherapy. Cancer Treat Rev 2007; 33:191-202.

Westerlund B, Nordlund P, Uhlin U, Eaker D, Eklund H.The three-dimensional structure of notexin, a presynaptic neurotoxic phospholipase a2 at 2.0 a resolution. FEBS Lett 1992; 301:159-164.

Zhai RG, Bellen HJ.The architecture of the active zone in the presynaptic nerve terminal. Physiology (Bethesda) 2004; 19:262-270.

Zimmerberg J, Chernomordik LV.Neuroscience. synaptic membranes bend to the will of a neurotoxin. Science 2005; 310:1626-1627.

van Meer G, Voelker DR, Feigenson GW.Membrane lipids: where they are and how they behave. Nat Rev Mol Cell Biol 2008; 9:112-124.